A Scanning Tunneling Microscope Control System with Potentiometric Capability

By

Adriaan H. Bredekamp

A dissertation submitted to the Department of Electrical Engineering, University of Cape Town, in partial fulfillment of the requirements for the degree of Master of Science in Applied Science.

Cape Town, July 2003.

Declaration

I, Adriaan Hendrik Bredekamp declare that this thesis, for my Master of Science in Applied Science at the University of Cape Town, is my own work and that I have given credit to the authors of documents where I have referenced them. I also declare that this thesis has not been presented previously to obtain any other qualification.

Signed: signature removed

Adriaan H. Bredekamp

Date : 22/7/2003

Acknowledgement

I would like to thank my supervisor, Prof. Jon Tapson (Department of Electrical Engineering, UCT) for his advice and guidance during this research project. Thanks are also due to Dr Candy Lang, who was always willing to explain some of the finer points of materials engineering.

I would also like to thank Mr. S. Schire for advice on some of the analogue circuit designs. A large word of thanks also goes to the staff of the "Glass house" for the large supplies of coffee that was always ready for consumption. Many thanks have to go to Peninsula Technikon and in specific Mr. Jan Ehlers for always having a couple of subjects for me to lecture.

The people at the University of Basel, (Michael, Simon, Alex, Luca, Silvia, Meike, Roland, Olivier, Andreas, Roberto, Julian and many more) which showed me what a scanned surface is supposed to look like. Thanks for teaching me lots of new techniques, tricks and help me to get much more out of the Swiss experience than what I expected. The work in Switzerland was not part of my MSc in anyway, but since the Institute of Physics is heavily involved in probe microscope, it was the perfect place to work for 3 years to learn more about STM.

A word of thanks to my family who supported me from 1999 onwards when I started this project. It took 3 years longer because of my additional learning experience in Basel, Switzerland where I learned everything I know about probe microscopes, but my family was always there for me.

Synopsis

This report starts by describing the background research and work that had already been done on the UCT scanning tunneling microscope (STM). This system is being developed in the Department of Electrical Engineering at UCT. It goes on to describe the continuation of the research work that was done for this dissertation on the STM at UCT. The work was originally started by Dr. Tapson for his PhD (1994), and continued by the author for his MTech degree in 1997 and 1998. The work was temporary discontinued from May 2000 till August 2002 to enable the author to work as a contract engineer at the Institute of Physics in Basel, Switzerland to learn more about the construction of probe microscopes.

The new work evolved around the need to implement scanning tunneling potentiometry (STP) capability in the new STM. This capability should give the end-user the capability of looking at the sub-surface structure of any material on a sub-micron scale. The basic STP function must be implemented in two dimensions in the plane of the specimen. The STM tip is then used as a highly localized voltmeter to sense what the potential distribution is at that point on the surface. The potential information that is obtained is then used to plot two images of the potential distribution over the surface in the X and Y directions. The topographic information is obtained in the usual way from the STM scan. This method gives three collocated images as the result and a better understanding of the surface structure is obtained in this way.

The penetration depth of the potential scan can be varied by adjusting the frequency of the applied AC signal in the X and Y directions. This use of the skin effect should allow the end user to obtain slices of the surface at various penetration levels of the specimen. These slices will give a picture of what happens from the surface up to a certain penetration depth. The interpretation of these images could be very difficult because the skin effect does not stop at a defined penetration depth. Only the 3 dB point is defined, which means that sub surface structures below the 3 dB point will also have an influence on the obtained image.

During the course of the research new hardware and scanning software was implemented to enable the error-free acquisition of new data. This entailed splitting the existing XY controller into three separate parts namely a Communications interface, and two STP measurement boards. This was suggested as one of the conclusions of the MTech thesis

results. The PC software stayed the same but for a change in the array size, that holds the acquired data. This was again changed after the work experience in Basel and is explained in chapter 6.

The review of all the work that was done previously is done in chapter 3. In chapter 4, the fundamentals of scanning tunneling potentiometry are reviewed along with a detailed explanation of what is expected from the results. This very important chapter covers the theoretical aspect of the thesis. This chapter also explains the working of both the 50kHz and the new 1MHz detector. Chapter 5 is explaining the working of the pre-amplifier and the reason for various noise sources associated with it. The following chapter explains the working of the embedded software, and hardware. The hardware and software went through two iterations during this MSc and the reasons for this is explained here.

This is then followed by a chapter on the results where the images that were obtained are discussed. In this chapter, a list of all the work that was done for this thesis is also listed.

Table of Contents

List of abbreviations

Å	Angstrom
ADC	Analogue to Digital Converter
AFM	Atomic Force Microscope
BTC	Binary Two's Compliment
DAC	Digital to Analogue Converter
dB	decibel
DC	Direct Current
DSP	Digital Signal Processor
EM	Electro-Magnetic
EMI	Electro Magnetic Interference
FIFO	First in, First Out
GUI	Graphic User Interface
i	Integral control constant
IBM	International Business Machines
IC	Integrated Circuit
Ir	Iridium
JPEG	Joined Picture Expert Group
k	Control scaling constant
kHz	kilohertz
LPF	Low Pass Filter
LSB	Least significant bit
mA	milliAmpere
MHz	MegaHertz
MS	Microsoft
MSB	Most significant bit
nA	nanoAmpere
nm	nanometer
p	Proportional control constant
PC	Personal Computer
PGA	Pin Grid Array
PI	Combination of *p* and *i* controller variables
Pt	Platinum

PWM	Pulse width modulation
PZT	Lead-Zirconate-Titanate
RF	Radio Frequency
Rh	Rhodium
SHARC	Super Harvard Architecture Computer
Si	Silicon
SMT	Surface Mount Technology
STM	Scanning Tunneling Microscope
STP	Scanning Tunneling Potentiometry
TIF	Tagged Image Format
USB	Universal Serial Bus

List of Figures

Chapter 1: Introduction

The first successful scanning tunneling microscope or STM was built in 1982 in the IBM Research Labs in Zurich, Switzerland. This new type of electronic microscope had the ability to obtain atomic resolution, and for the first time materials scientists had the ability to image atoms in their lattice structure using a tabletop size instrument[1, 2]. It was no longer necessary to use very powerful electron microscopes (which could fill a room) to get atomic resolution. In 1986, the scientific community recognized the achievement of Binnig and Rohrer of IBM by presenting them with the Nobel Prize in Physics[3].

It was a long and sometimes difficult road to get to the design of the first STM. Russel Young of the National Bureau of Standards in the USA realized that it is possible to get better resolution than available from an electron microscope by using the tunneling effect[3, 4]. This quantum mechanical effect allows an electron to cross a barrier, which according to classical physics it cannot cross, since it lacks sufficiently high energy. It makes its way so to speak through a potential mountain by quantum-mechanical tunneling; hence the name tunneling microscope. This means that if a conductive scanning tip is near enough to a conductive surface (10 Å, i.e. 3-4 atom diameters) a current will flow even at low voltages. Young did manage to build an instrument but only managed to obtain a resolution of 200 Å. This resolution was thus considerably poorer than other electron microscopes of that time.

Binnig and Rohrer succeeded with their STM[1,5] but it was still very bulky. One cause of this was the vibrational isolation system that was used to isolate the scanner from disturbances in the environment. The microscope was built on a permanent magnet that floated freely on a disk of superconducting lead. Today, less bulky and equally effective isolation mechanisms have been developed[6,7]. The Nanosurf Company of Switzerland has developed an STM and recently an AFM (Atomic Force Microscope) that are good examples of this[8]. The horizontal resolution was approximately 2 Å and the vertical resolution was 0.1Å for the Nanosurf STM instrument. In 1986, Pohl defined the required lateral resolution to be 0.1 Å and the vertical resolution to be 0.01 Å [9]. This is the typical resolution required to operate with atomic resolution.

The STM is a very simple instrument when considered in terms of its basic components. The primary component is the piezo ceramic scanner element into which a wire tip is fixed. The tip can be a piece of noble metal wire (Pt 15% Rh or Pt-Ir alloys) that protrudes out of the scanner tube. The movement of the scanner is controlled by a computer that gives out control voltages that are applied onto the scanner to cause controlled movements in the X and Y direction. To sense the topography of the specimen surface, a control loop tries to maintain a constant current between the surface and the sample. The Z control voltage is then plotted to reveal the surface features of the sample.

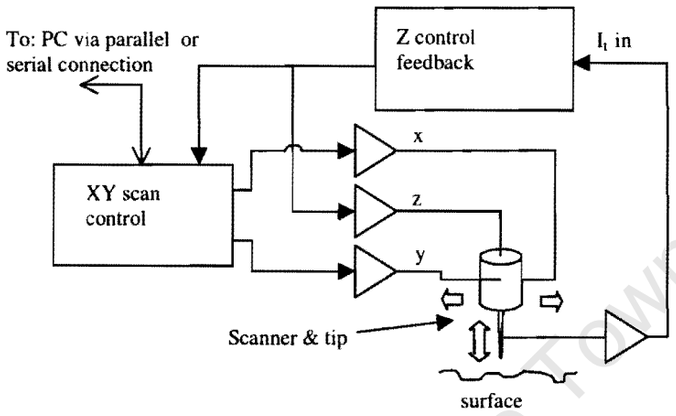

Figure 1.1: Block diagram of our STM system – showing the scanning tip and scanner from which the tunneling current is amplified and used as the input to the height feedback controller. The output of the Z controller is fed to high voltage amplifiers along with the X and Y signals from the XY scan generator to the scanner and tip. The Z control loop output is also sent to the XY controller from where it is sent to the PC for display.

Since 1982, there has been a considerable amount of new work done in this field, with surprising results. A whole group of sub-types has emerged from this single STM design. Instead of using current as a feedback variable, capacitance can be measured[10], as well as resistance, elasticity, magnetic force and a host of other variables. Resistance can be measured by applying a voltage across the sample, and measuring the current orthogonally to the electric field. This is called scanning tunneling potentiometry (STP) [11]. Elasticity measurements can be done using an atomic force microscope in which a stylus is used to profile the surface[12]. In these techniques, the micrometer scale deflections of the AFM stylus can be measured using a focused laser beam.

The addition of a resistiometric measurement capability in a scanning tunneling microscope (STM) is required for the application of this particular STM. In scanning tunneling potentiometry (STP) the tip is used as a highly localized probe for potential measurements on a conducting surface[10,13]. During a STM measurement of the surface topography, the surface is biased at a constant DC voltage, but during a STP measurement, a varying surface potential must be applied across the surface that must be measured. The varying surface potential is caused by regions of differing surface resistance, such as the grain boundaries of the material. The requirements for STP are as follows.

1. A signal must be applied across the surface, which will cause local points of differing surface potential.

2. A system must be included for distinguishing between the variations in tunneling current caused by topographic changes in the Z direction, and variations caused by local changes in potential.

Our system was designed to drive large high-frequency currents through bulk metal specimens. The addition of a transformer to step up the current before applying it to the surface of the sample is critical in this respect. This transformer coupling allows us to float the AC potentials on the DC bias. The result of this is that currents in the specimen plane of up to 1A are possible. In addition, the use of synchronous detection of the AC signal reduces the noise levels of the potentiometric information.

This thesis is about the implementation of STP capability in the STM at UCT[13,14]. The modifications include a bigger frequency range. The main aim is to prove that high frequency STP is feasible and to develop the hardware to test this scientifically.

Chapter 2: Review of STM technology

2.1 Introduction

There are various routes to improving the performance of a STM. By redesigning the controller electronics, it is possible to make it faster and more intelligent. The signal processing can be improved, in terms of the way it corrects a distorted image, or cancels environmental noise. The instrument size can be reduced to make it more compact[6]. The scanner hardware can be redesigned to accommodate different scan heads, or different tips. The system cost can also be reduced to make it affordable for universities and small research companies[7]. Every field related to STM is open to improvement.

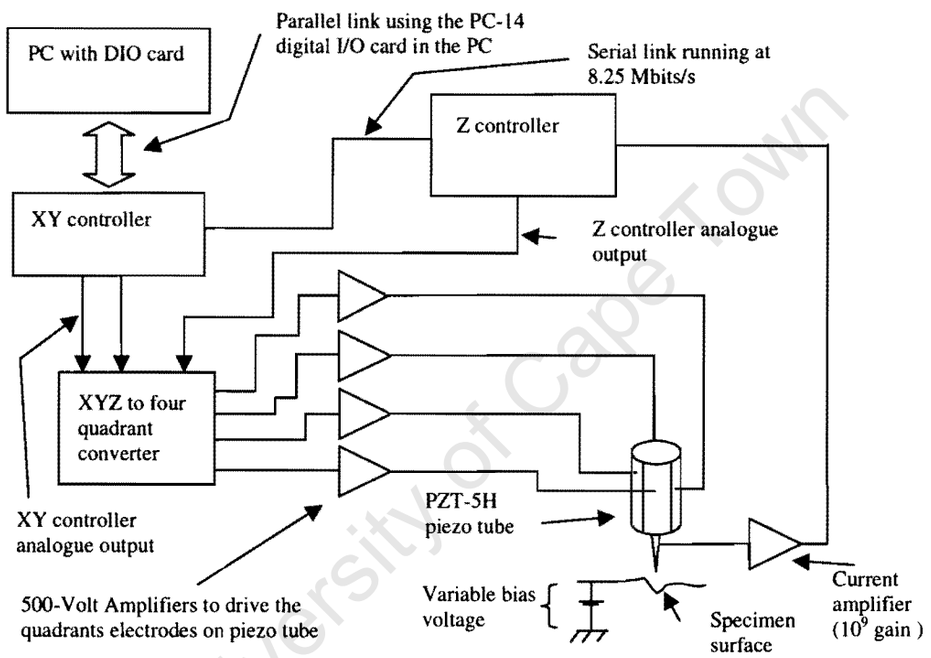

Figure 2.1: Block diagram of our existing STM system – showing the computer with the PC-14 card, the bi-directional parallel link running to the XY controller, the analogue outputs of the Z and XY controllers that go to the XYZ to 4 quadrant converter, the four 500 Volt amplifiers that drive the piezo tube, the 10^9 gain stage that amplifies the 1nA tunneling current and feeds it to the Z controller, and the variable voltage on the specimen surface.

2.2 The tunneling tip

Almost all of today's STM instruments use some kind of piezo ceramic scanner to scan over the surface to obtain the image. The tip is normally a piece of noble metal wire that protrudes through the hollow centre of the piezo tube. There are also several other ways of mounting the tip. It can be mounted in such a way that it is still protruding through the hollow centre, but when the specimen is scanned, a piezo tube lengthening or shortening will give a Z direction movement for the tip. Lateral deflections of the piezo material will give the X and Y tip movement. This method of mounting the tip can be used when the surface features are very rough and a large scan area is required. The scan area will however not be square in shape, but rather a long strip. Three separate piezo tubes or bar elements can also be used to mount the tip. In this case, each piezo tube is used only in the lengthwise direction. As each of the three piezo materials contracts or expands it produces the required movement in the XY and Z directions [1,8].

The tip is brought into close proximity to the surface (approximately one nanometer) of the specimen at which point a current (of the order of nano-amps) will start flowing from the surface to the tip. The bandwidth at the tip can be controlled in the XY direction, and is normally in the range of several kHz. There are however exceptions to the rule. One exception is the design of an optical switch type STM tip[15], which is discussed below.

2.2.1 Opto-electronic tip design

The optical switch type STM tip was designed to give very fast temporal resolution. These tips are used primarily for the measurement of laser induced transients on transmission lines and photoconductors[16]. These opto-electronic tips are also used to scan very fast over a small area to make a movie of the movement of atoms in their lattice structure[17]. The opto-electronic tip was designed to try to increase the scan speed of a STM.

The basic structure of these special tips is a PtRh wire tip that is attached to a photoconductive Si switch. A laser beam is focused through the substrate to control the conductiveness of the silicon switch. The time between the laser pulse being applied and the tip current flowing is then measured to obtain the required information about the specimen that is being scanned.

2.2.2 Tip sharpness

Tip sharpness is very important. When scanning at atomic resolution the surface features are created by atoms. This means that it would be ideal to have a single atom at the apex of the tip. If the tip is that sharp, the stream of electrons from or to can be considered to be from a single point. If a single atom is at the apex of the tip, then the tip can be modelled mathematically and the current can be characterised[18]. If the tip is not atomically sharp, it is possible to get tunneling currents forming at different points on the tip. The result of these haphazard tunneling points is that it is not possible to determine with great accuracy what the tip was imaging, and the result is a useless image, if an image was obtained at all. It is thus important to take good care of the tip and to understand the geometry of the tip[19].

There are many sources in the literature on how to prepare very sharp tips by etching and/or cutting[20, 21,22]. Most of these tips last about an hour before they start to go blunt again. This is normally due to oxidation of the surface of the tip, or tip crashes. Tips are made out of Pt-15%Ir or Pt-Rh alloy. The basic process of etching involves an etching solution and some mechanism to pull the etched wire from the solution at a constant rate. A typical rate is about 1mm per minute. This process gives tips that can have only a few atoms at the tip. Commercial tips are available with only one atom at the tip, but these tips are very expensive[23]. These are manufactured using a combination of etching and polishing.

2.3 The control system

The loop that controls the height above the specimen surface is the most important part in the whole system. This loop has to maintain a constant height above the surface by keeping a tunneling current value constant. In this lies the first problem with the height control loop. It is designed to control the current while it is actually intended to do something totally different. It must control the height above the surface of the specimen. It has only a superficial correspondence with the widely used *single-input-single-output* control loops. The problem is to decide what the tunneling current represents. Is it the input to the control loop, or is it a disturbance that is added to the system? Tapson[13] also noted this ambiguity.

There are various ways of implementing a PI controller for the height control above the specimen[24,25, 26]. Tapson covered the complete development of control systems in his thesis[13].

Tapson's work came down to a decision between using a sampled data system or an analogue system. The design of an analogue scan system tends to be more favoured by research groups[27, 28]. Commercial instruments tend to use digital control systems. An example of this is the *Discoverer* system from Topometrix[23]. Another example is the *CryoSTM* system from Oxford Instruments[29]. The drawback of a digital controller is that it is more complicated to build. Not only the software, but also the physical circuit design and layout take up time. The only way to avoid the software design problem is to use a hardwired digital controller. This was done by Valenzuela-Benavides[28]. This hardwired controller can be classified under the same heading as the analogue controller because once the controller parameters are built into the system, it is very difficult to change. It is better to go with a system where the control parameters can be easily changed in software.

The capability to change the control parameters in a digital control system makes the overall system very flexible. It is possible to scan a broad range of specimens without rewiring the controller; only the software parameters are changed. The decision for a digital control system can be subdivided further between a digital signal processor (DSP) system and a microcontroller-based system. The use of a DSP based system is very popular because DSP algorithms are very powerful[30,31]. These powerful processors allow the implementation of any type of control strategy from a simple PI loop to a more complex multivariable or fuzzy control loop[32].

The other option to follow in a digital control system is to use a microcontroller based system. This was done by the present author[14,25] and by Tapson[13]. The microcontroller solution has two possibilities. The first option was used by Tapson and consists of generating a lookup table as a substitute to calculating a real-time algorithm. The lookup table is calculated with a control algorithm on a PC or workstation and is downloaded to the microcontroller. The advantage of this is that the microcontrollers are very cheap and very fast throughput rates are still possible. The downside is that the lookup table download is time consuming. The table must also be recalculated each time the specimen is changed. A second option is to use fast microcontrollers. This is the route taken by the present author. The XY and Z directional control is done by the microcontroller. The Z algorithm is calculated after each sample and a throughput comparable to a DSP is still obtained.

The use of floating point calculations in the control loop was later questioned by Tapson[33]. The control loop is an *integer-in-integer-out* loop. The use of a DSP processor to do the floating-point calculations in the control loop is thus questionable. The ADC and DAC values can all be represented by integer values. The calculations will produce fractions, but they will be rounded off if integer mathematics is used. The control bandwidth requirement of a STM is also low enough in the Z direction that a fast microcontroller can handle the control loop with ease[25].

2.4 Imaging systems

The imaging systems that were used in the earlier STM systems were mainly analogue storage oscilloscopes. The actual image was then photographed from the screen of the storage oscilloscope to get a hard copy of the image that was scanned. This was a cumbersome method at best. Later years brought combinations of data display, e.g. using both a storage oscilloscope and a PC[34]. In even later years, the various researchers and companies started to use personal computers to do the image display of the specimen surface[24,27,30,31,35,36]. This is the method that is still used today[25,37]. Some researchers have tried to use a different method of obtaining the image with the aid of sophisticated frame processors and frame grabbers[38]. This was done to try and improve the throughput speed of the STM.

Most early STMs used the MS-DOS based operating system to display a line type image. Some early papers show examples of line type images[39, 40,41]. The lines then formed a type of 3-dimensional display that represented the topography of the surface. With the popularity of MS Windows[42] products, Windows became the operating system of choice to do graphical displays of the data. A good example of this is Barchesi *et al,* who used a Pentium based computer system (PC) and Visual Basic under Windows to develop their application[43]. Some companies like Topometrix[23] have used Unix based systems, and others have opted for a Windows based modular software approach using Labview[44], eg. Oxford Instruments[29].

2.5 Review of STP technology

The basic requirement for scanning tunneling potentiometry is:

1. A signal must be applied across the surface, which will cause local points of differing surface potential.

2. A system must be included for distinguishing between the variations in tunneling current caused by topographic changes in the Z direction, and variations caused by local changes in potential.

Muralt and Pohl[11] used a system that was optimised for the study of metal-insulator-metal structures. This type of surface had a high likelihood of showing a high resistance at the grain boundaries. The topographical signal was then detected using a demodulator that consisted of a lock-in amplifier to separate the AC signal from the DC signal. The DC signal was used for the feedback in the Z direction to keep the height above the specimen surface constant. This system worked well.

The system of Kirtley *et al*[45] measured the topographic and the potentiometer information in a sequential method. The topographic information was measured and then the feedback control was disabled for a short time to take a potentiometric measurement by using a spatially varying DC signal. This system claimed a SNR improvement of at least 10 times over the system of Muralt and Pohl[11].

The system of Pelz and Koch[46] used an AC signal and a square wave bias voltage to obtain the topography and the potentiometric information at the same time. The topography was measured only when the bias voltage was high and the potential measurement by means of a lock-in amplifier when the bias voltage was low.

All these methods used a surface potential gradient in only one direction, which meant that assumptions had to be made as to the electrical connectivity perpendicular to the varying potential[11,45,46,47].

Chapter 3: Previous work at UCT

3.1 Introduction

The only STM related work that was done previously at UCT was by Tapson[13] and by the author[14] during his MTech studies at the Cape Technikon. The Materials Engineering Department at UCT needed a wide area STM that could be used for metallurgical research. Tapson designed and build a STM that filled that requirement. A new control system was then implemented by the author along with faster scan rates and new user software that runs under Windows.

3.2 The STM

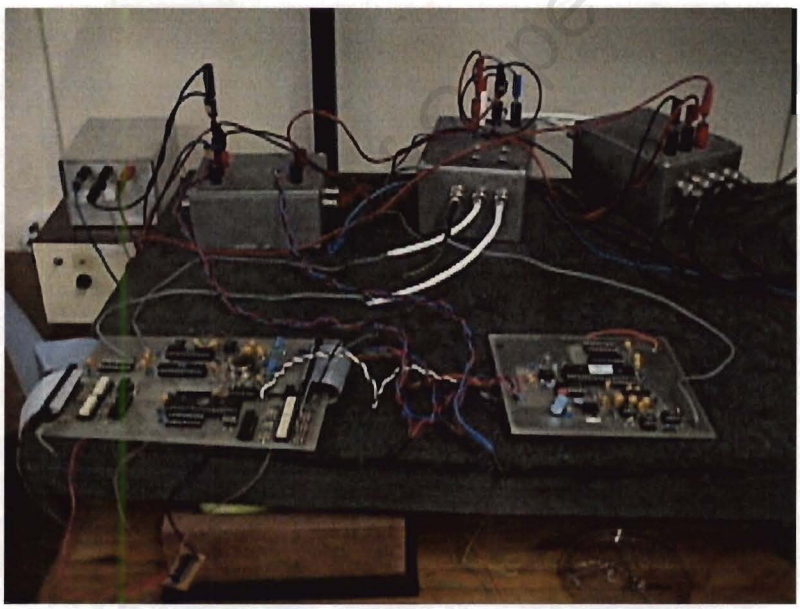

Figure 3.1: Photograph of the scanning tunneling microscope, showing the XY and Z controller in the foreground. In the background from right to left, are the 500V amplifiers, the XYZ to four-quadrant converter and the three power supplies, all resting on the vibrational isolation assembly. The two wires (X and Y) from the XY controller and the single wire from the output of the Z controller can be seen going to the XYZ to four-quadrant converter and then to the 500V amplifier from where the four signals can be seen emerging again.

The STM consists of several essential components that make up the system. These are the scan head, the control electronics, the PC and the vibrational isolation assembly. The scan

head is mounted on the vibrational isolation assembly to isolate it from various kinds of movement. These include minute micron size building vibrations, vibrations caused by footsteps and even accidental bumps into the STM instrument as a whole.

The control electronics is mounted outside of the PC to make it easy to isolate it from electrical and electro-magnetic noise. It is here that the analogue-to-digital (ADC) and digital to analogue (DAC) conversions are performed.

3.2.1 Scan head

The scan head is the same head that was used in the previous iteration of the STM[13]. It consists of a PZT-5H piezo ceramic scanner tube that is mounted inside a steel block. The block has set screws that are used to do the coarse approach of the tip to the sample. In the scanner tube is mounted the scan tip (usually a Pt-Ir wire). The tips can easily be damaged, but it is easy to sharpen them again[20,21,22].

On top of the steel block is mounted the first (transconductance) amplifier that converts the tunneling current to a voltage and which amplifies the voltage by 10^6.

The steel block with the scanner tube rests on a second steel block onto which the sample is mounted, and which contains the fine approach screw. The fine approach screw has a micrometer screw gauge thread with a pitch of 0.5 mm per turn. The block is suspended with rubber bands from the vibrational isolation assembly.

3.2.2 Vibrational isolation

The vibrational isolation assembly was constructed to isolate the STM head from any mechanical vibrations. These vibrations can be anything from micron size vibrations of the building caused by the wind or passing vehicles, to accidental bumps into the STM table. The isolation consists of a set of three rubber bands that suspend the scanner head from the scanner mount. The mount rests on a 5-millimeter sheet of foam rubber. The STM mount is covered with a bell jar to prevent movements of the scanhead by the surrounding air. The

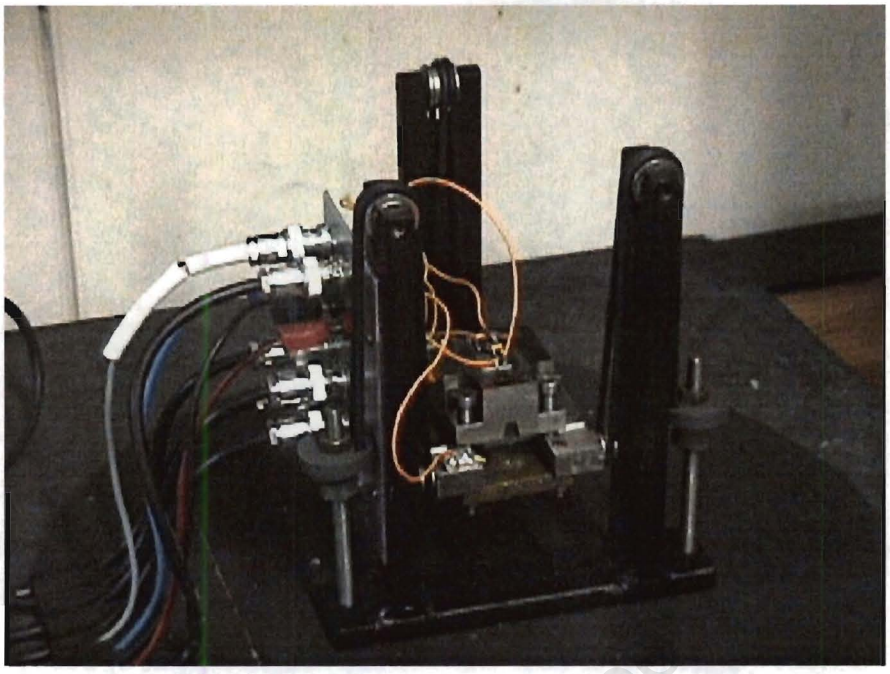

Figure 3.2: Photograph of the scanhead on its suspension rig. The scanhead with the 10^6 amplifier can be seen clearly along with the wires that connect it to the BNC connectors. The cables on the left supply the power to the 10^6 amplifier and the control signals to the piezo tube.

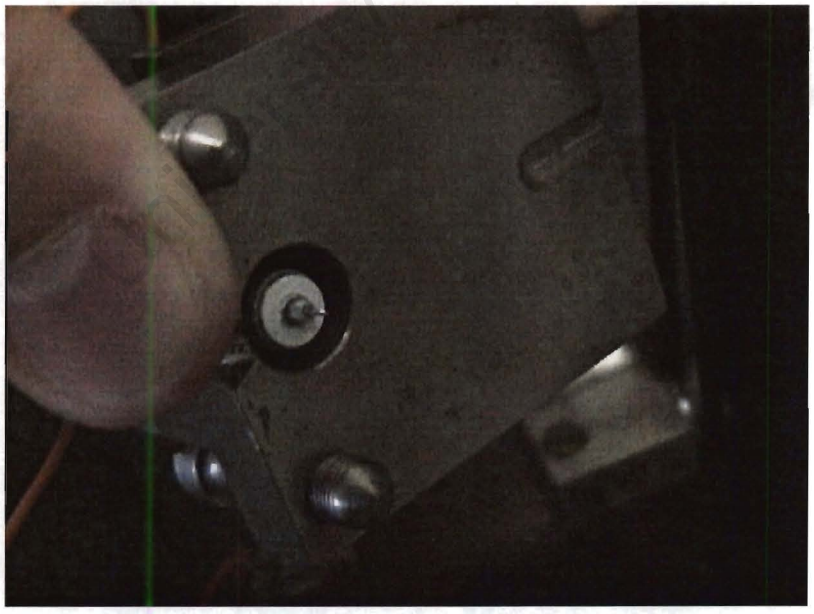

Figure 3.3: Photograph of the scanhead from the underside. The tip and the piezo tube can be seen protruding through the steel block.

whole assembly rests on a very heavy slab of slate, measuring 5cm by 50cm by 100cm. The slab makes the assembly very heavy and helps to dampen any frequency that the assembly is exposed too. The slab is supported at its corners by four sets of five tennis balls. This has the effect of blocking most if not all of the received vibrational energy. The tennis balls are contained in four tennis ball buckets, which hold five tennis balls each. The tennis ball buckets rest on some more sheets of foam rubber.

This setup has proven to be effective in the previous STM in removing most of the mechanical vibrations that might prevent the obtaining of good images[13].

3.3 Electronic systems

The electronics of this study consist of the scan head, the PC, the control boards for the XY and Z controllers, and the various power supplies. The scan head needs a 500V power supply to drive the piezo tube and a ±15V supply for the 10^6 current gain amplifier and the 10^3 voltage gain amplifier.

The control boards give out the XY and Z directional control voltages that are first split into a four-quadrant signals before being passed to the 500V amplifiers. The outputs of the 500V amplifiers are then used to drive the four quadrants of the piezo tube.

3.3.1 XY controller

The XY controller as it is shown in figure 3.1, was implemented by the author[14] as an improvement to the system used by Tapson[13]. The XY controller scans the tip in a raster pattern over the sample with a movement bandwidth of 3.3kHz. Our XY controller, which has two 16-bit DACs to give the required lateral resolution, was implemented using a PIC17c43 microcontroller. By incrementing the two 16 bit DACs by different amounts the image magnification factor can be controlled. A scan size from 5nm × 5nm up to about 5µm × 5µm is achieved.

The XY controller also communicates via two optically isolated parallel ports to a PC. One parallel port is used for transmitting and the other for reception of data from the PC. The ports are optically isolated to prevent noise coming from the PC analogue ground line from

reaching the embedded system. It was shown in the previous iteration of the electronics, that ground line noise was a problem[13].

The PC was running Windows NT 4 and the imaging software was written in MS Visual C++. The two parallel ports were implemented using an 8255-type slot-in card in the PC. The control software on the PC communicates to the XY controller various parameters such as the magnification factor and control variables. The Z controller also requires some of these configuration parameters. The PC configures the XY controller, which then configures the Z controller before each scan is done.

The speed of throughput between the PC and the XY controller was improved by using a custom device driver. It was found that when the slot-in card was controlled from the user program level the throughput was in the order of 40.3 kbytes/s. If the control lines and data reads were controlled by the device driver and not by the user program, the throughput improved by a factor of 3.23. The received data was then passed up as a 1024 byte array through the NT security layers to the user application program in the case of data control by the device driver.

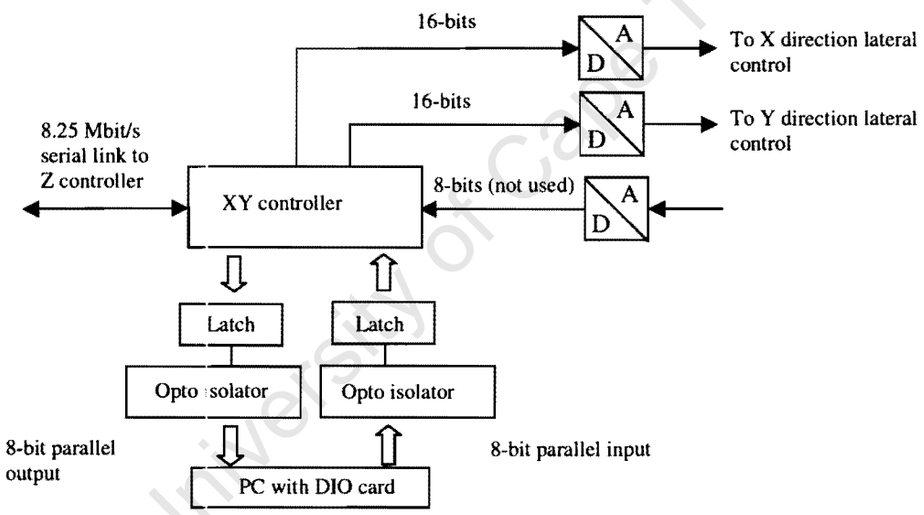

Figure 3.4. XY controller block diagram, showing the 16-bit X and Y DAC outputs and one of the 8-bit STP inputs. From the XY controller the data is sent to a latch and then to the PC via a parallel link that is implemented with an 8255-type card in the PC. The serial link to the Z controller can also be seen.

3.3.2 Z controller

The existing Z controller was implemented by the author as part of his MTech thesis [14]. It is important to note that the Z controller implements a PI (proportional - integral) control system:

$$Z_{out} = k(i_e.p + k_I \int i_e \, dt) \quad (1)$$

where k is a scaling constant, p is the proportional constant, k_I the integral constant and i_e the error current. If we take the first-order digital approximation to this:

$$Z_{out}(n) = p.i_e(n) + [Z_{out}(n-1) + k_I.i_e(n)] \quad (2)$$

then the control system is an *integer in – integer out* system. It must be noted at this stage that there are several ways of implementing a first order PI control loop. The accuracy obtained by using floating-point calculations is not needed, negating one of the basic advantages of the DSP approach. (It has recently been shown that the use of integer variables in the control loop is fundamental in eliminating limit cycling, which is a substantial source of errors in this application[13]). It is however easier and cheaper to implement the Z control loop on a microcontroller.

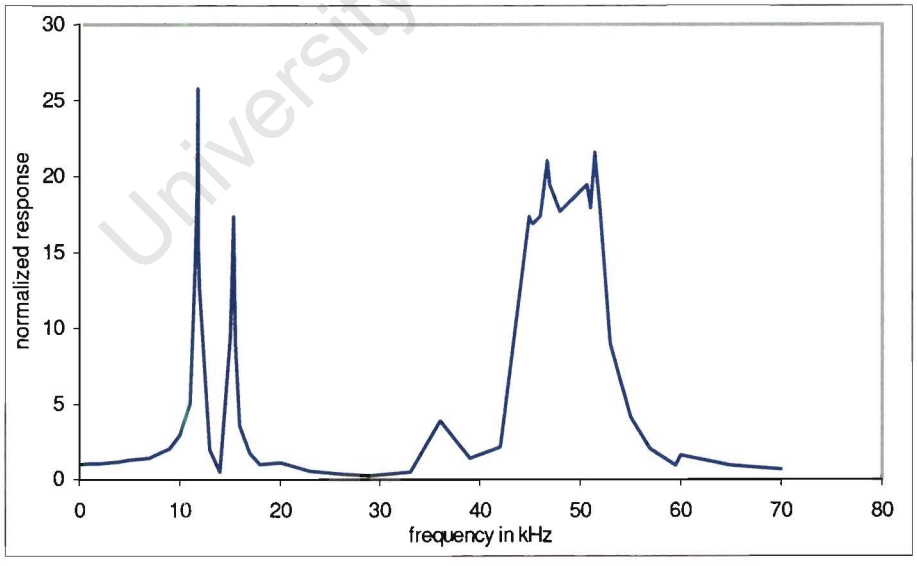

Figure 3.5. This graph shows the first resonant peak at around 10 kHz of the PZT-5H tube that is mounted in the scan head. The piezo tube can only be controlled up to a third of this frequency[13].

The error current input to the Z control system (i_e) is digitised using an 8-bit ADC. The setpoint tunneling current is of the order of 1 nA. For a very small change in tunneling distance, a large change in current can be expected; hence, 8-bit resolution is more than adequate. The measured current is then subtracted from the setpoint current to give the error current i_e in the algorithm shown above.

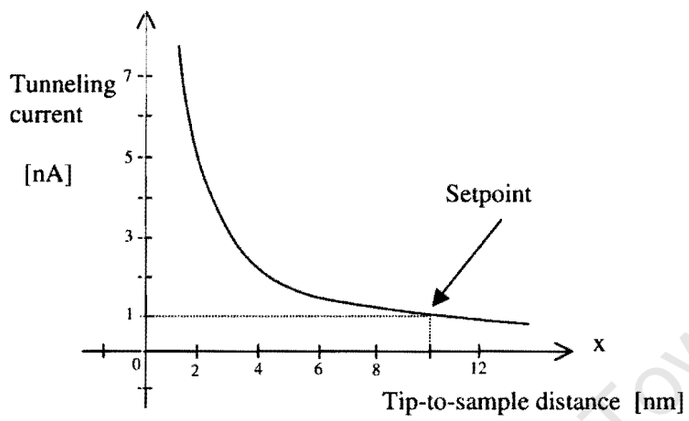

Figure. 3.6. Typical setpoint on the tunneling current vs. tunneling distance curve.

The output value of the loop ($Z_{out}(n)$) is passed to a 20-bit DAC and also fed back into the control loop as $Z_{out}(n-1)$. The 20–bit resolution is required to meet the requirement of 0.01 Å in the Z direction (given that the full scanner range is at least 1μm). This fine output resolution also helps to reduce limit cycling and co-operative behaviour [32]. The DAC output has a third order low pass Butterworth filter with a cut-off at 60 kHz. The filter is needed because the digital controller is a discrete in – discrete out system. The DAC output has an unavoidable zero at half the sampling frequency (the Nyquist frequency). It is frequency folded at the Nyquist frequency, hence a post-sampling filter on the output is required.

The Z controller in our case was implemented using a 33MHz Microchip PIC17c43 controller, with an 8.25 Mbit/s synchronous serial link running to the XY controller. The programming of the PIC microcontrollers is simplified by their RISC instruction set. The previous implementation[13] used Intel 8051 based controllers, which had over 200 assembler

instructions compared to the 58 of the PIC17cxx series. The Microchip PIC series can also implement a synchronous serial port that has speeded up communications between the two processors.

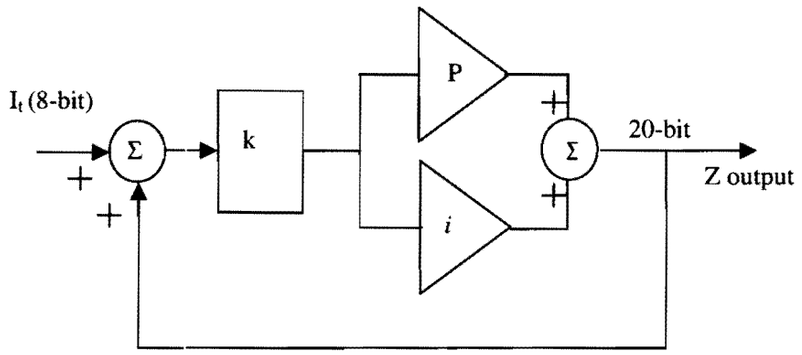

Figure 3.7. The Z algorithm, showing the PI control loop, 8-bit current input from the tunneling junction and the 20-bit output to the piezo tube. P is the proportional gain constant, *i* is the integration constant and k is an offset adjust constant.

During any scan only a very small fraction of the full 20-bit range is used to scan the surface. It is only during the tip approach stage that the tip is fully extended. This is because no tunneling current is measured and the control system tries to compensate by extending the tip to contact the surface to get a current reading. The coarse distance approach is done by hand with a very fine pitch screw movement. An oscilloscope is used to see when a tunneling current is obtained at which stage the user can configure the PC to do a scan.

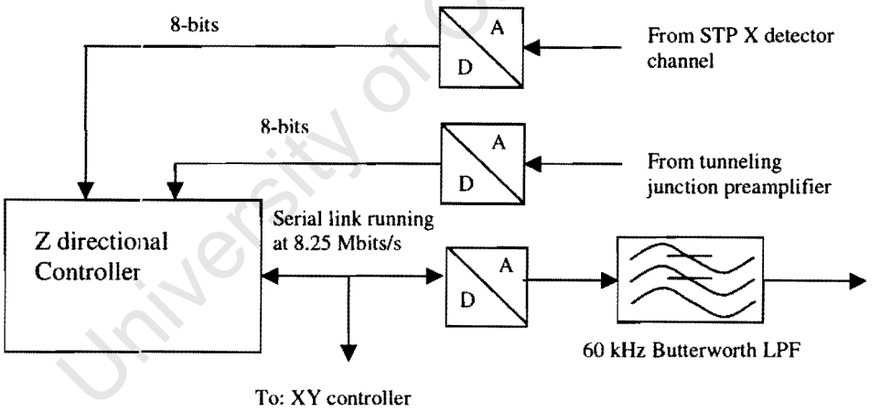

Figure 3.8. The Z controller block diagram, showing the data inputs and the DAC output with the 3rd order Butterworth LPF. The high-speed serial link is common to the DAC and the XY controller.

The Z controller software loop executes in 13.3µs (75kHz) and a software delay is added to bring the speed down to 60 kHz. It can thus be seen that a fast microcontroller can do the Z directional control as well as a DSP system, but at a fraction of the cost.

3.4 DSP implementation

The previous work[14] was concerned with the implementation of a new control and imaging system. A literature study was done to determine the best solution for a DSP based control system implementation. First, an off-the-shelf system was looked at, using plug in boards that are available from *Data Translation*[48] and *National Instruments*[44].

The *Data Translation* board was designed to plug into a standard PC. It had a TMS320 DSP type processor with dual port memory and various DACs and ADCs onboard. It could easily be programmed in C to control the STM. It was decided not to use this well designed plug in board because of its very high cost, which was outside the available budget for the MTech thesis[14]. The placing of the analogue circuits in the PC is questionable since the PC produces a lot of electrical switching noise. The ADC and DAC circuits on these cards may at best be good up to 12 bits unless the analogue circuits are very well shielded. It is better to place the analogue circuits with their controllers outside the PC in a shielded box.

It must be noted that with all the available software that a company like *Data Translation*[48] and *National Instruments*[44] offer, it is possible to build an off the shelf system but at very high cost. This system might be easy to develop because of the visual block diagram based programming language of Labview[44].

The next option was to use a small DSP development board that is available from Texas Instruments[49]. These use the TMS320c30 processor with some outside logic, a DAC, an ADC and a serial port. The system was too restricted to allow easy interfacing to a STM system. The DSP chip had the speed to run the system fast enough, but was lacking in the environment that it was built into, namely the development board. It was available at a relatively low cost. A paper that became available near the end of the author's work confirmed that this option was the wrong path to follow. Paillard *et al*[37] used a TMS320c50 development board that is the same as the one that the author considered except for a more powerful DSP processor. The results that they obtained for their Z directional controller gave

only a sampling rate of 25kHz. It must be noted that the onboard ADC and DAC were used, which were optimized for speech processing. Paillard also noted that the DSP processor still had lots of spare processing capacity. The system was priced at US $250.00, which is too expensive when it was compared to the cost of producing the PCB with the microcontroller, ADC and DAC to form a Z controller. The cost of the latter worked out to about $65.00.

A second DSP system was also evaluated. The Analog Devices SHARC 2106x development board is a very capable system[50]. This board was available at US $179 and came with the C compiler, C libraries and a simulator. It was finally also not selected because the cost in developing the PCB for this DSP chip would have been too high.

3.5 Multi processor system

A multi processor system using cheap microcontrollers was also considered. In this configuration, each processor is given a simple task to do. The tasks are coordinated by inter processor communications or handshaking. The advantage of a multi processor system is that the control process can be chopped up into many pieces to give each processor a simple task to do. The processors can then communicate with each other to determine which is doing what. In this manner a parallel execution of instructions is obtained without using a fast processor that does time slicing to simulate a parallel process.

In the context of the STM system, a parallel process would occur when the Z control algorithm is running and data is read from the XY control system without an interruption to the Z control algorithm's execution.

The choice for the final selection was between an Intel 8051 style processor[51] and the much faster Microchip PIC17 series of microcontrollers[52]. Other microcontrollers were not considered because the development tools for these two processors were readily available and the author was familiar with these two products. The final choice was based on the fact that the Microchip PIC series have more peripherals available on the microcontroller, and that the development tools were available from the Microchip company free of charge. This was a major selling point of the Microchip product.

The PIC17c43 devices that were selected for the project had several features that made them very suitable. The most important feature was the 8x8 bit unsigned multiplier that can multiply two bytes in a single machine cycle. This was very useful for calculating the Z directional control algorithm in real time. The second important feature was the high-speed serial port, which can be used in a synchronous mode. In this mode, it generates a data stream with a clock signal, which is what the serial 20-bit DAC requires for its input. The third feature was the 16 bit wide external bus that was used to load the 16-bit DACs for the X and Y directional signal generation. The PIC17 series is also capable of doing low-end DSP functions[53]. The PIC17 series of microcontrollers are therefore ideal for this kind of application when the system was originally designed in 1997[14].

In the previous STM design, the embedded system is only divided between two processors, but it was further divided to make some parts of the system easier to work with and to correct some design errors. If the communication to and from the PC is separated from the XY control system, a third processor could perform it. The X and Y control processes can also be split to put yet a fourth processor in. The inter-processor communications can manage the synchronization of the data, but the communications protocol will probably be very complex to program. This is described in more detail in chapter 6 where the splitting of the system into 4 controllers is discussed.

3.6 Hardware Results

The results of the hardware design were mixed. Several faults were discovered during the testing procedure and corrective action was implemented to minimise the effect of these problems. Each one of the potential problems and solutions is discussed below.

3.6.1 Timing problem

Each component of the hardware was tested and an unfortunate hardware-timing problem was discovered on the XY controller during the previous study[14]. The write pulse that the PIC microcontroller generates during its 'table latch write' operation is only 30ns long which was 20 ns to short to drive the Burr-Brown DAC712 16-bit DAC. This problem can be overcome by lowering the clock frequency of both XY and Z controllers to 20MHz.

The reduced sampling frequency for the Z controller means that the control loop bandwidth was reduced to 42kHz for the unoptimized code. The code was optimized at the beginning of the MSc project and the 60kHz Z scan update rate was achieved again.

3.6.2 Opto-Couplers

It was found that the opto couplers for the XY controller were not fast enough to give good square shaped waveforms at 100kHz. The opto coupler used was the 4N32. This opto coupler uses a Darlington pair for an output stage. These opto couplers were changed for 4N25 devices, which use only a single BJT transistor for their output stage. Slightly better results were obtained with the 4N25. They were still not good enough because the waveforms began to lose the square shape around only 40kHz. A future design should then use fast digital opto isolators like the 6N137, which can handle a data throughput of 10Mbit/s.

Again, it was decided not to implement the new digital opto-couplers straight away, but rather to wait and do all the corrections at the same time in a completely new PCB layout. The cost of producing a single double sided through hole plated board is in the region of R200,00 and it is therefore not a good idea to build new PCBs for every discovered mistake. The 4N32 and 4N25 devices are pin compatible, but the 6N137 is not pin compatible with the existing PCB layout. The new PCB layout will also split the XY controller into three parts. This is described in more detail in chapter 6.

3.6.3 PC-14 card

The parallel port communications bus formed a major bottleneck. The problem here is more software related than hardware related. The Windows NT system has too many security checks before the information gets down to the hardware level, or from the hardware level, to the user level. The second part of this problem is that the Eagle Technology[54] software is written to comply with a wide range of hardware and is not designed with high throughput speed in mind. The Eagle software is called by functions from the Visual C++ or Visual Basic software that the programmer uses. The only feature of the Eagle software apparent to the user, is an include file with the function names in it.

The hardware was tested and a throughput of only 250 Hz was obtained with the Eagle EDR software under Windows NT 4. The throughput calculation is a bit arbitrary here because it is

taken as the time taken for a low to high to low transition on the output of the card. This 250 Hz throughput figure shows up as a 125 Hz oscillation on an oscilloscope. It was found that if the debug information was removed from the Visual C++ program, then the hardware response increased from 250 Hz to 300 Hz. The obtained throughput rate with the EDR software was unacceptable for the embedded-system-to-PC data link. The software support section of Eagle Technology said that this is an expected figure for the configuration that was used. The configuration that is referred to here is the combination of Windows NT and the Eagle software. Eagle's software support said that the throughput would have been a lot faster under Windows '95. Windows NT was however chosen as the operating system for this study because it is a lot stabler than Windows '95.

At this stage, a cursory investigation was made of the PC-14 card and it was found that with the available hardware it should be possible to run the card at speeds in excess of 1MHz. This ruled the hardware out as a possible cause for the low throughput.

Windows NT uses a system of device drivers to communicate between different levels of the operating system. It is possible to write data straight to any memory location in a Windows '95 system. In Windows NT, the operating system will simply not allow this memory write operation without working through a device driver. Improving the throughput of the card required a new, purpose-specific device driver to be written. The test software that was developed along with the device driver proved that the throughput could be as high as 50kHz on a 166MHz MMX Pentium machine that was used by the device driver programmer. If the port-write-routines for the Intel 8255 chips that make up the PC-14 card are hard-coded in the device driver itself, the throughput jumps up to 550 kHz. This 550 kHz shows up as a 275kHz oscillation on an oscilloscope. Hard-coding the port-read and write routines in the device driver means that the code is in the device driver and not in the user program. The data that the device driver collects during a data scan, can then be sent as an array up through the NT security layers from the device driver to the user level. The user only gets the results and does not control the actual read routine. Most of the software had to be rewritten to accommodate the new device driver based interface to the PC-14 card. This means that all the EDR software had to be removed from the existing STM scan software.

On the 486 DX4-100 MHz machine that is used for the STM development the speed of the later method drops to 170 kHz due to the difference in hardware design between the two

generations of PCs. The way that the 550 kHz throughput and the 170 kHz throughput on the PC were obtained is to just switch any port on the PC-14 card on and off as fast as possible. These numbers are arbitrary and are just used to learn more about the capability of the system under test.

It was found that the opto couplers had insufficient bandwidth, as was mentioned previously. The PC-14 card will read in different values due to the deformation of the waveform. The problem was solved by doing several reads of the port and only taking the last read as a valid read. The throughput that was obtained was 12.3 kbytes/s with the handshaking signals between the PC and the embedded system included. The read sequence is delayed by a factor of three and the three bytes are then assembled in a double word. On a Pentium 166 MMX, the speed should be 3 23 times faster at 40.4 kbytes/s. It would however be restricted to a throughput speed of about 12kHz because of the signal deformation of the 4N25 opto-couplers. It must be noted that the 12.3 kbytes/s throughput on the existing system is enough and no more speed is really needed. It would however be good to send other information to the PC, such as also like the actual value of the tunneling voltage or the position of the tip in the X and Y space. These features are again not required for the operation of the STM, but would be good to have in a future iteration of the hardware and software.

The factor of 3.23 is derived from previous testing and is an empirical number. If the device driver is used to just switch a port on and off, a throughput of 550kHz is observed. This drops to 170kHz on a 486DX4-100.

If the opto-couplers are replaced, the device driver can be recompiled to do fewer reads on the device driver level and give an even faster data throughput. The data is then just read once instead of three times. This means that the 40.4 kbytes/s will jump up to 121.2 kbytes/s on a 166MHz Pentium based machine. The 121.4 kbytes/s throughput is an absolute maximum for the system and is dependent on the bus speed of the PC that is used and the device driver read sequence.

3.7 Recommendations from the previous work

The best way to implement a fast, low cost STM control system in hardware would be to split the XY controller into more parts. This will ease the computational load on each processor

and still keep the cost down. The alternative is to implement a DSP processor. This means that the XY DACs and the communications part must be split. Ideally, the X and Y controllers must also be placed separately.

The next generation of the X, Y and Z directional controllers should be very carefully designed to minimize noise in the system. It would be best to construct the whole system inside a metal enclosure. The individual components can also be built inside their own metal enclosures and all power and signal connections can be made via shielded cable. An example of this would be to enclose the sensitive DAC output and filter stage of the Z controller in a separate metal enclosure that is mounted on the PC board.

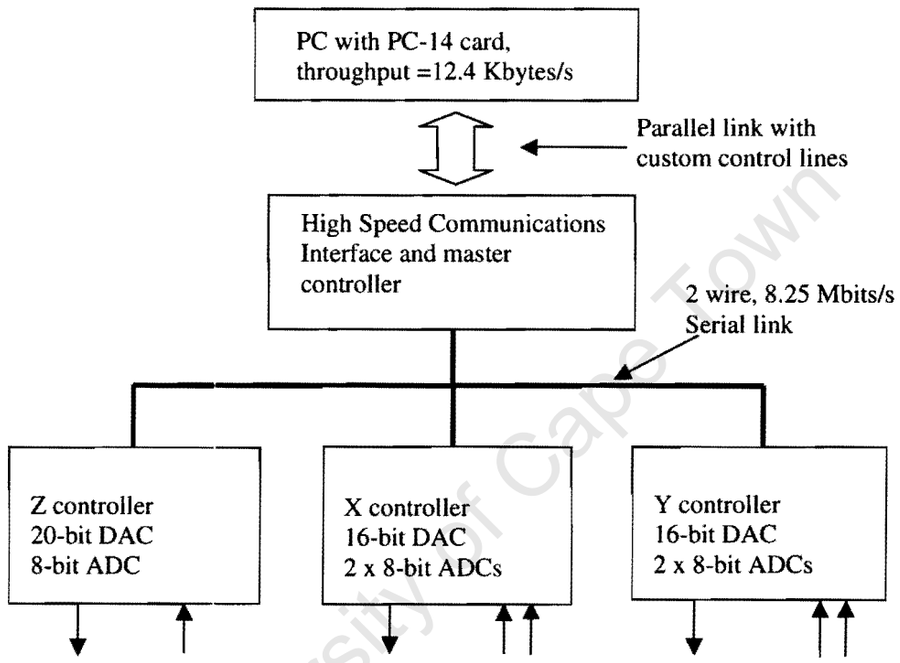

Figure 3.9: Block diagram of the proposed system that will replace the existing XY controller. The system is split up into a high-speed interface that does the communications between the PC and the various sub-systems. The Z controller stays the same from the previous iteration, but the X and Y control signals are now generated from two separate control boards. The X and Y control boards are supplied with two 8-bit ADCs each to implement a possible image correction algorithm or an STP function.

3.8 Software Results

The results for each section will be considered separately. The software was the most important section of the MTech thesis and it took the longest time to complete. The more complex the software, the longer it took to get it working properly.

3.8.1 The Z controller

The Z control loop is only 119 instructions long and the result is that it is very easy to program and test.

The main problem that was found with the Z directional controller software was when the input clock frequency was lowered to 20MHz from 33MHz. The reason for the lowering of the clock frequency was due to a hardware-timing problem. The DAC712 chip required a write pulse of minimum 50ns in duration at 33MHz the PIC was generating a pulse of width 30ns, which is to short. The resulting problem was that the execution speed of the Z directional controller dropped to 42 kHz from 69 kHz.

The splitting of the XY controller will have the indirect effect of bringing the clock speed of the Z controller back up to 33 MHz and thus the control loop execution speed back up to 60kHz.

3.8.2 The XY controller

The amount of data that the XY controller has to handle, coupled with the amount of signalling in the 3 kHz time frames, is the downfall of the XY controller. The XY controller has to do the X and Y code generation for the raster pattern and write it out to the 16-bit DACs. It has to receive 20 data sets of three bytes each from the Z controller, which have to be kept or discarded. The 20^{th} set of three bytes must be transmitted to the PC.

It was found that the existing XY controller slows the whole system because it has to do too many tasks. The XY controller should be split into three separate components, namely separate X and Y controllers and a high-speed interface that controls them and does the complete PC interfacing.

3.8.3 The PC software

The PC software is working satisfactorily and achieved the goal of providing an environment for viewing the data and using the STM with ease. It also provided easy storage and retrieval of data, and the facility for easy upgrading of the PC software. This is done by means of object-orientated programming.

3.9 Recommendations on the software

Several problems can be solved with the next version of the STM software. Both the embedded software for the Z and XY controllers, and the PC can be improved. The main software upgrades are described below.

3.9.1 Embedded system

The PIC microcontroller software was written to produce software modules that can easily be used to create new software for the STM embedded system. It is suggested that the X and Y control is done on separate microcontrollers. The X, Y and Z controllers will then be controlled by a master controller that will also do the interfacing to the PC.

The communications interface can be equipped with a circular buffer to hold the incoming data from the Z controller. It will keep sending the data from the buffer unless it has some other housekeeping tasks to do.

3.9.2 PC software updates

The PC software has only the very minimum of functionality. The online help file system must still be constructed along with a better system for setting the various variables of the STM. It is possible to place menu options that are used a lot on the shortcut menu list, or to make the menu available with a click of the secondary mouse button.

More functionality can be added by using the functions that are available via Matlab. These would include converting the image from raw data to a TIF or JPEG formatted image. A colouring scheme can also be added to show differing heights. It is also highly recommended

that the line-scan type image be transformed into a relief type image. This type of image will show the surface topography better.

It is also possible to program the embedded system to restart itself without a reset by just forcing the controller to wait for a download when it has finished scanning the required number of data points.

The bottom line with the PC software is that it needs a lot more functionality and the way the information is presented must be improved.

3.10 Conclusion from the previous work

The combined effect of this was that cheap processors could be used while still maintaining a very fast execution time for the embedded system. The cost of the two PIC17c43 processors with their "glue" logic was still below the cost of a single DSP processor when this system was originally designed in 1997[14]. Currently with new technology, it is not the case anymore because the price of DSP processors has dropped to the level of $2 per piece. The performance advantage comes from the ability to make the system modular. In this way components like the XY controller can be removed and replaced with a different module, without redesigning the rest of the system.

Chapter 4: STP implementation

4.1 Introduction

This MSc dissertation is about the implementation of the full STP capability in two dimensions and at high frequency, with the associated control and scan electronics. Currently the STP circuit operates at 50 kHz; this must be upgraded to at least 1MHz with a later iteration. The reason for this is to make use of the skin effect to try to obtain a sub-micron image of the material structure below the surface of the specimen. As the frequency increases (of the voltage applied across the surface of the specimen) the penetration depth of the current decreases. By decreasing the skin depth, with increasing frequency, it is possible to take progressively thinner "slices" through the material of the specimen. By combining these different images, a three dimensional image of the sub-surface structure of the material can be generated.

There is no instrument in the world that can do the tomography at the moment. The use of a transmission electron microscope (TEM), will give you the structure of the bulk of the sub-surface structure, but not a three dimensional image. The STP technique has potential applications in the semiconductor industry.

4.2 Implementation of STP

During STP measurements, if a DC bias is used for the tunneling current, the tip position (in the Z direction) becomes dependent on the tunnelling voltage at that point on the specimen surface. The control loop compensates by adjusting the tunneling distance so that the correct tunneling current is flowing again. This means that a change in potential would not be distinguished from a variation in specimen height. The contributions from AC components can however be easily separated out from the tunneling current. The DC current component that is extracted from the tunneling junction is used to obtain conventional topographic information. The following four figures show the effect of an AC and DC bias on the surface of the specimen. The specimen surface shows an electrical field distribution on the surface that can be measured by the STM tip.

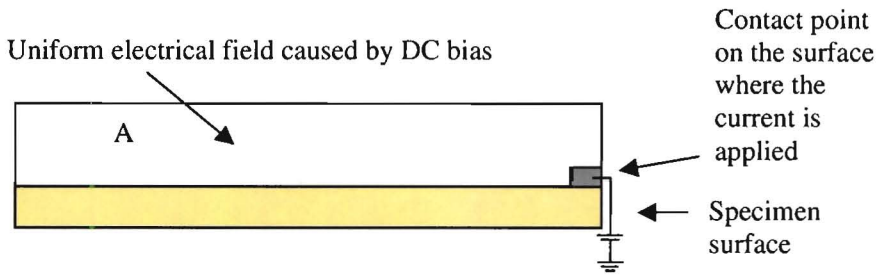

Figure 4.1 Effect of a DC bias as it is used in STM topography scans. The area 'A' is an electrical field caused by the bias.

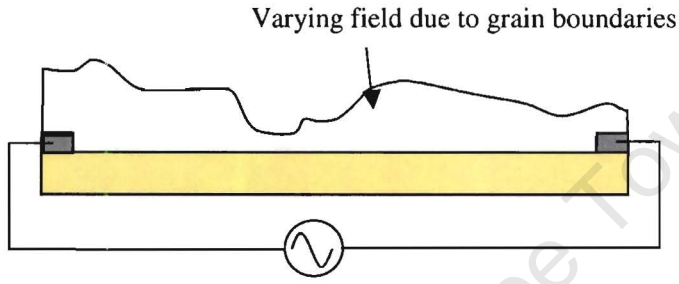

Figure 4.2 The effect of an AC bias across the specimen surface. The electrical field is caused by the grain boundaries in the material, which has a resistance to the current flow in the material. The AC bias has two contact points on the surface of the specimen; hence there is a current flow across the surface.

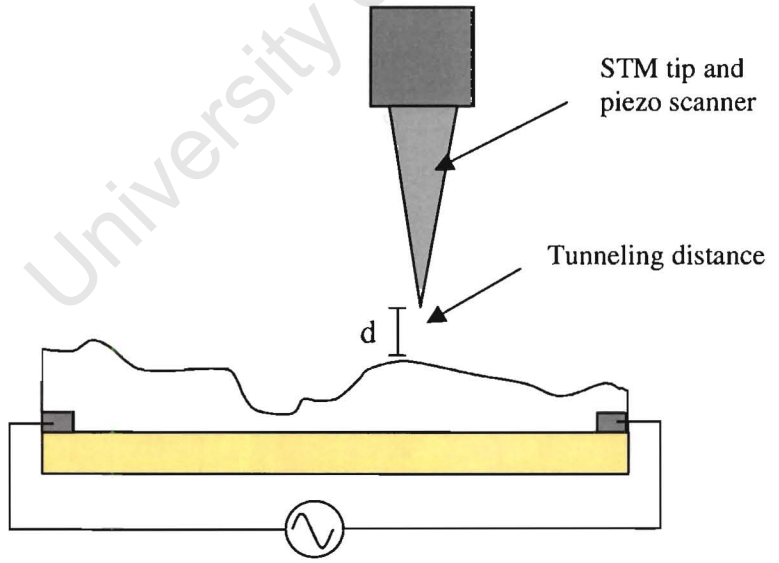

Figure 4.3 The effect of an AC only bias on the Z feedback loop. The Z controller does not "see" the topography of the surface of the specimen, but rather the electrical field caused by the grain boundaries in the material. This causes the controller to settle at what it thinks is a distance(d) above the surface corresponding to a 1nA current flow between surface and the tip.

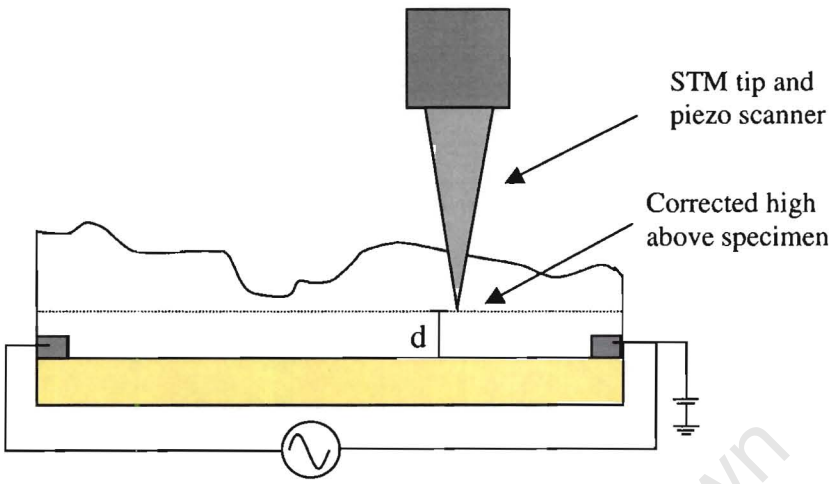

Figure 4.4 The effect of a DC and an AC bias over the surface of the sample. The Z controller filters out the AC component and only uses the DC bias to determine the correct distance(d) above the surface of the sample.

The usual way of doing STP is only in one direction on the surface plane. An assumption has to be made as to the electrical connectivity of the sample surface in the direction perpendicular to the varying voltage[11]. The direction in which the AC signal is applied may not be the direction that contains the best potentiometric information. An example of such a problem material is graphite. By applying a second electrode perpendicular to the first set in the plane of the specimen, and applying a slightly different AC signal to the AC signal across the sample, scanning tunneling potentiometry in two dimensions can be done[55,56,57]. This set-up creates a set of signals that is orthogonal. In our system, the first AC signal is at 50kHz and the second is at 51kHz. The two applied signals are at different frequencies to enable the synchronous detector to distinguish between them.

The frequencies for the STP were chosen to be as high as possible to enable maximum use of skin effect. Skin effect increases current flow close to the surface, which causes the surface potential to more closely reflect the near surface potentiometric information rather than the bulk resistance. The potentiometric information for both the X and Y directions are extracted simultaneously using a demodulation circuit. This is shown in Figure 4.5 along with the electronic implementation of one of the channels in Figure 4.6.

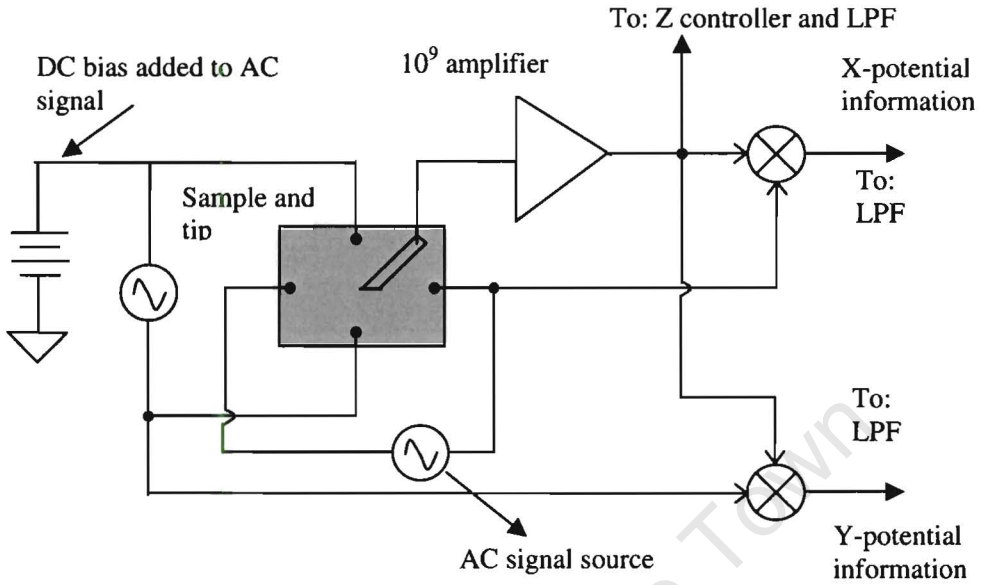

Figure 4.5. The configuration of the STP circuit. The application of two spatially orthogonal signals across the specimen surface can be seen. The same tip is used to simultaneously measure the DC and AC components of the tunneling current before signal processing.

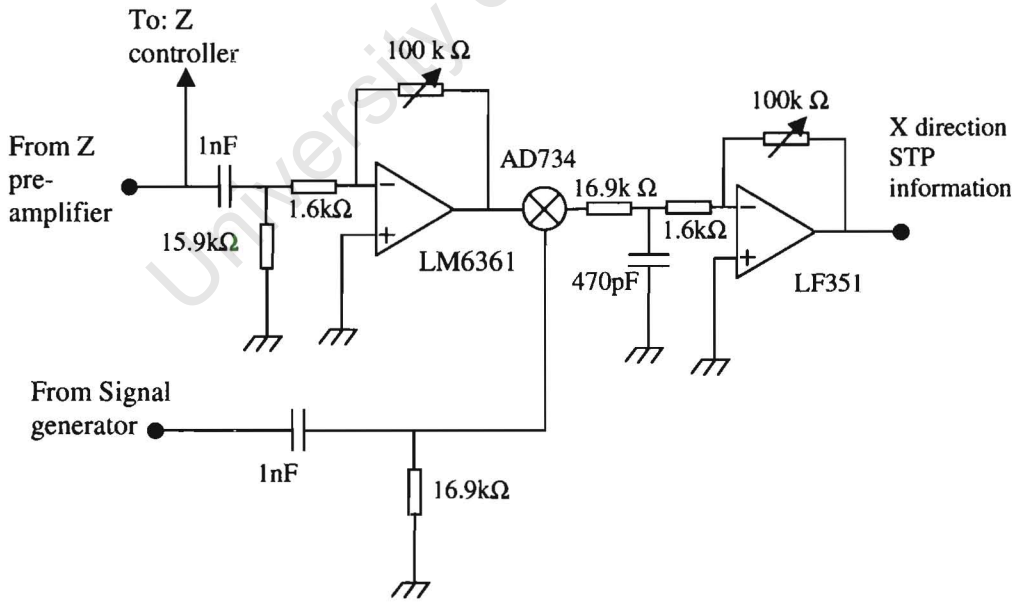

Figure 4.6 Drawing of the X channel of the 50kHz STP circuit. The high pass filter on the input of the detector circuit can be clearly seen. This is followed by an amplifier and an analogue multiplier that multiplies it with the signal generator signal. This is then low pass filtered and amplified again before it is digitized by the ADC.

The diagram in Figure 4.6 requires some more explanation. The signal from the Z pre-amplifier contains both the DC and the AC components of the signals that were applied to the specimen. The STP analogue detector circuit requires only the AC part. For this reason, a high pass filter can be added that blocks the DC. The cut-off frequency is 20kHz in this case, because the lowest applied AC signal is at 50kHz, hence anything below a half of the lowest applied STP frequency can be filtered. The AC input of the detector is then amplified by a factor of 100 using a wide band LM6361 op-amp. That output is then fed into one input of the analogue multiplier. The other input for the AD633[50] multiplier comes from the signal generator that is applying the orthogonal potential to the sample. The multiplication process produces various products at the same time, only the required signal must be retained and the rest must be filtered out. The required output from the analogue multiplier is a difference signal, but the process also produces a sum of products signal. The sum and difference can be explained as follows, where potential A comes from the tunneling pre-amplifier and potential B from the associated signal generator:

$$Y = [A \cos(\omega_1 t + \phi_1)] \times [B \cos(\omega_2 t + \phi_2)] \quad (3)$$

Where ω is the frequency of the signal and ϕ is the phase of the applied signals, and A and B the amplitude of the applied signals. This is multiplied together and reduces to

$$Y = \tfrac{1}{2} A B [\cos(\omega_1 t + \phi_1 - \omega_2 t - \phi_2) + \cos(\omega_1 t + \phi_1 + \omega_2 t + \phi_2)] \quad (4)$$

A low pass filter is used to remove the right hand term, and we are left with only the difference term.

$$Y = \tfrac{1}{2} A B [\cos(\omega_1 t - \omega_2 t + \phi_1 - \phi_2)] \quad (5)$$

$$= \tfrac{1}{2} A B [\cos(\alpha t + \delta)] \quad (6)$$

For small phase differences and a small difference between the applied frequencies, $\cos(\alpha t+\delta)$ is approximately equal to one. This leaves only

$$Y = \tfrac{1}{2} AB \quad (7)$$

The B signal is applied from the signal generator and is constant in amplitude; however the A signal is a detected signal and any change in the amplitude of 'A' will be due to the desired potential contrast in the specimen.

The applied signal from the signal generators can vary from 50 kHz to 1MHz as long as the signals are orthogonal. This means that at the output of the analogue multiplier, a (2 kHz) low pass filter can be added to get rid of the sum and product signals. The signal is then multiplied again by a factor of 100 to get it into the range of the analogue to digital converter that is used to sample the signal. The only difference between the 50kHz and the 1MHz detectors is the actual multiplier that is used. For the 1 MHz detector, a high frequency multiplier must be used, such as the AD734 instead of the AD633.

A first detector was constructed on Veroboard using the AD633 analogue multiplier. It was only tested up to 50kHz since the multiplier IC has a bandwidth of 1 MHz. Results for this circuit are presented in Chapter 7. The second multiplier circuit was constructed using an AD734 analogue multiplier. This IC has a bandwidth of 10MHz. The second detector was placed on a PC board with lots of shielding in the form of shielded cable, and a massive ground plane. Like the STP measurement boards, it was also made compact enough to fit into a standard shielded metal box. A photo is shown in Figure 4.8.

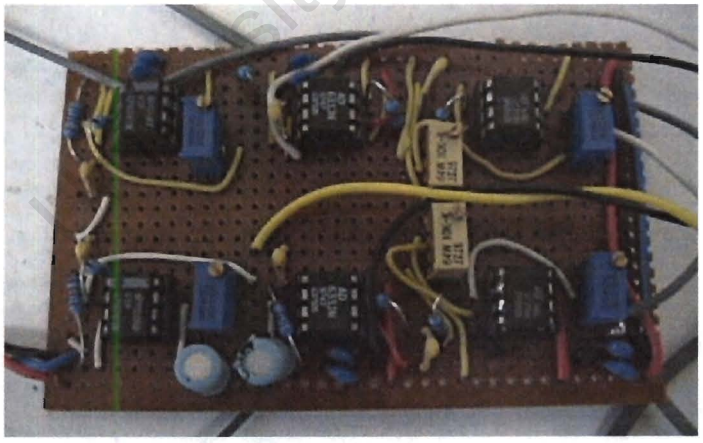

Figure 4.7 Photograph of the AD633 based STP detector that was built on Veroboard. The signal comes in from the left-hand side and is first amplified, then multiplied before it is amplified again on the right hand side. Both X and Y channels are shown; the X channel is the top row of components.

Figure 4.8. Photograph of the AD734 based 1MHz detector. The wires are attached to the terminal blocks to help with easy removal of the PCB from the enclosure. The 10^3 Z pre-amplifier is also included on this board to improve the signal distribution. It is visible on the left side just above the large cluster of capacitors. The diode banks on the right-hand side are there to ensure the signal is kept below the 5 volt input threshold of the sampling ADCs. The two AD734 multiplier ICs are visible as the 14- pin devices to the right of the photo, one for the X channel and one for the Y channel.

The second multiplier was only tested to ensure that the power connections and signal pathways are working, but was never tested as part of a STP system. This was due to time constraints placed on the author. The board is however operational and will give low noise results when used in a future iteration of the system. This thesis was meant to only prove the concept of high frequency STP. Both the STP detector circuits that is shown in figure 4.7 and 4.8 consists of 2 channels, one for X and one for Y. The connection diagram for 2 channel STP can be seen in figure 4.5.

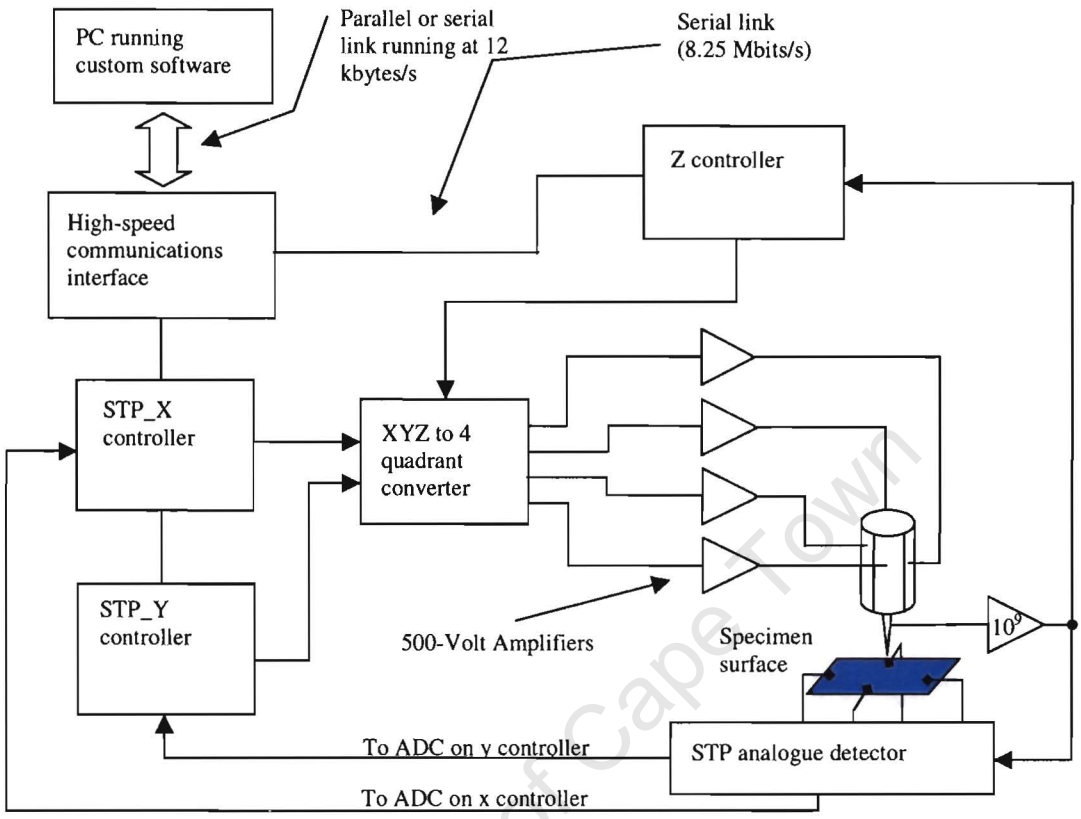

Figure 4.9 Position of the Analogue detector in the STP measurement system. This diagram shows the complete STM/STP configuration of the system. This can be compared to Figure 2.1, which only shows the STM configuration.

4.3 Skin effect re-visited

By changing the frequency of the potential that is applied across the surface, the penetration depth of the current can be controlled. The signal wavelength becomes shorter as the frequency increases. When this signal is applied to a specimen, the signals beyond a certain point are attenuated rapidly giving rise to the skin effect. The skin depth is a measure of how deep the current penetrates into the surface of the material. The calculation for the skin depth first defines attenuation constant α.

$$\alpha = \sqrt{\pi f \mu \sigma} \tag{8}$$

where f is frequency in Hertz, μ is the permeability of the material and σ is the conductivity of the material in S/m.

The skin depth is then simply defined as

$$\lambda = \frac{1}{\alpha} \qquad [m] \tag{9}$$

A graph of the skin depth for various materials is shown in Figure 4.10. The values for the permeability and the conductivity are available in standard tables. The drop off in skin depth can be seen clearly with an increase in frequency. In Figure 4.11 the frequency range from 100kHz to 10 MHz is shown in more detail. The high range of the frequency from 1MHz to 10 MHz clearly shows that the skin depth has not yet reached zero.

From Figure 4.11, we can determine the useable range of frequencies for the STP scans. If we look at the graph for silicon, we see that at frequencies above 1 MHz the curve is quite flat. There is thus no point in using frequencies above 1MHz because the reduction in penetration depth is very small.

The modelling of penetration depth will be complicated if a mixture of materials is used. This might be the case in a metal insulator composite. For example, the curve in Figure 4.11 shows that the 3 db point of gold and silicon at 100kHz differ by about 50μm. This must be kept in mind whenever an image set in the X and Y directions is analysed. STP gives different information at different frequencies and with different materials.

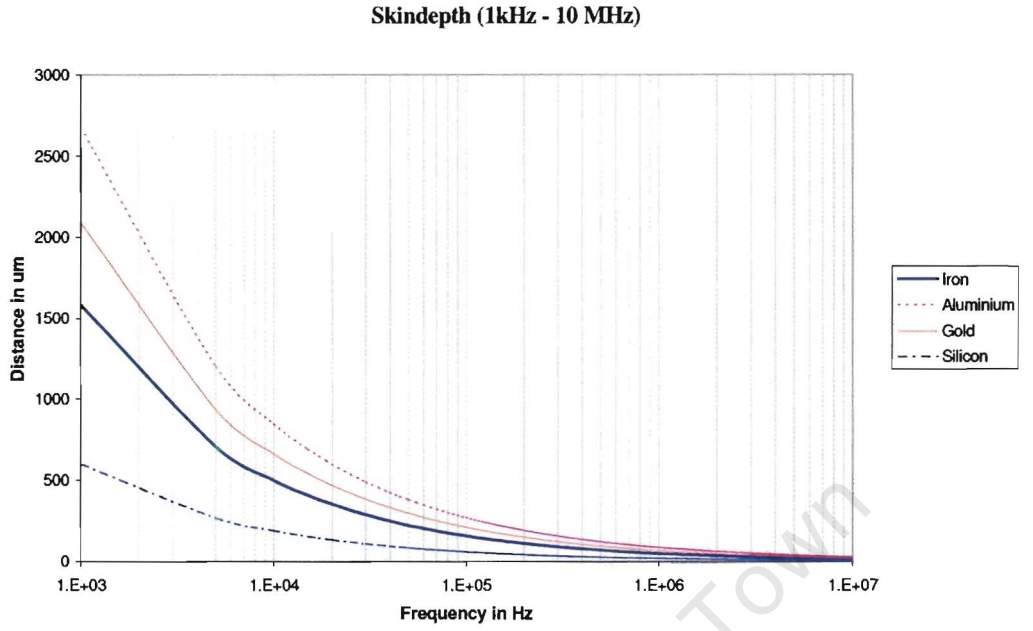

Figure 4.10 Graph of skin depth versus frequency. The decrease in skin depth can be clearly seen for an increase in applied frequency.

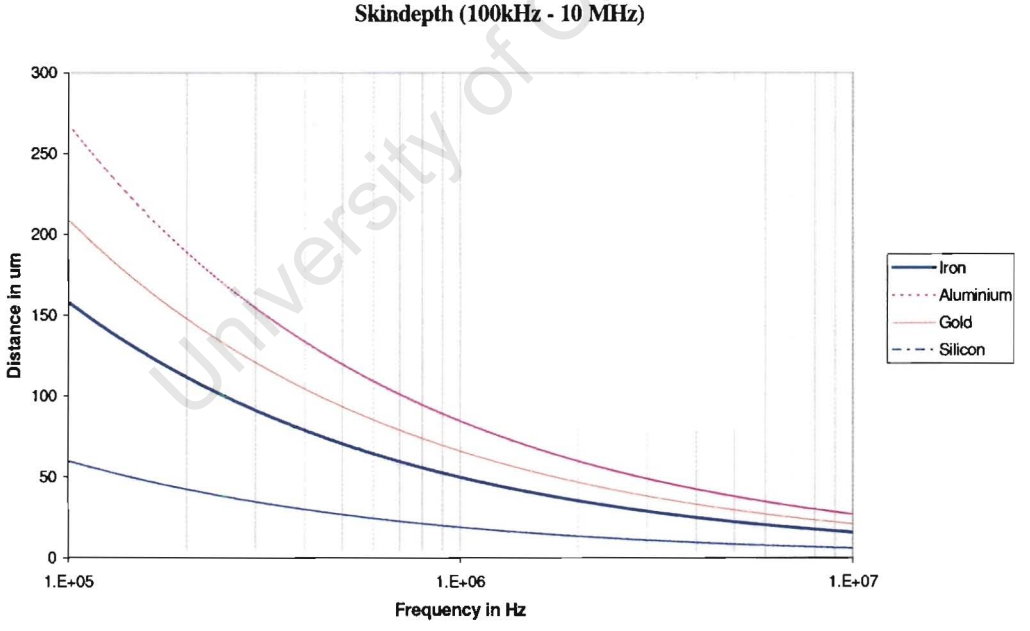

Figure 4.11 The frequency range from 100kHz to 10 MHz clearly shows a usable range for the application of the STP technique. Above 1 MHz, some materials like silicon show only a small decrease in skin depth for a large change in frequency.

4.4 A simple model of STP tomography

A simple model is presented below to highlight some of the issues in STP and tomography. This explanation can also be used as a basis for interpreting the images that will be presented in Chapter 7.

In the first image we use a low frequency and hence have a high penetration depth. The STP scan should show something similar in the top view. It must be noted that the blob on the right side of the top view is due to a small grain in the material. If it is compared to Figure 4.13, it is seen that the top view of the grain on the right side is unchanged. It would probably be impossible to determine whether the little circular grain on the right side is as it is shown or whether it is a tubular structure in the side view. A tubular structure will show up as a circular blob on the top view in both the low and high frequency cases.

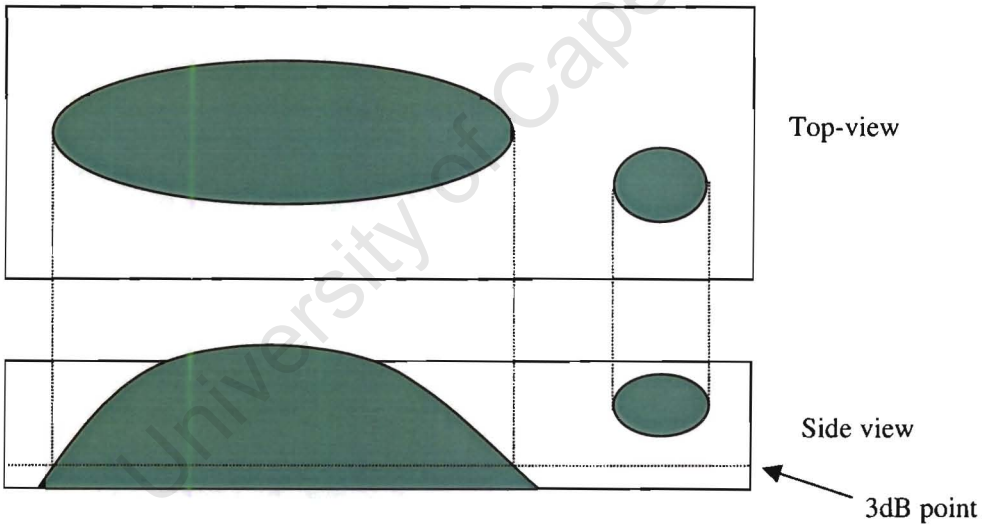

Figure 4.12 This is a possible image (top view) that might be obtained from the STP system. The side view of the specimen is also shown to show what sub surface structure will cause the obtained top view. This image is for a low frequency and a high penetration depth.

It must be noted that the horizontal line that is used to indicate the depth of penetration is actually the 3dB point of the signal that is applied over the surface. The -3dB or half power point is an engineering term to indicate at which point the voltage level has dropped to 0.707 of its original value. The implication of this for the image processing is that there will be information below the 3-dB point that makes a contribution to the scan of the surface. It is

likely that similar features would produce different strength potentiometric information if they were at different depths in the material.

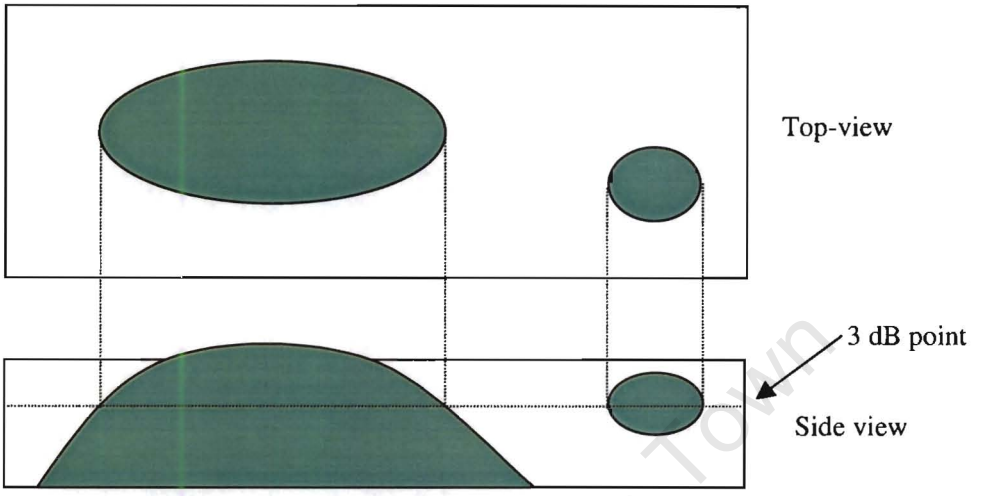

Figure 4.13 This shows a possible image that could be obtained from the STP circuitry. In this case, we have a high frequency and a lower penetration depth than in fig. 4.12. Note the apparently reduced size of the feature on the left

In short, a STP scan of the same area, but at different surface frequencies would produce different information. This extra information has to be interpreted very carefully because of the complexity of the AC current penetration into the material, and the subsurface connectivity of the material.

4.5 Conclusion

This project will continue the investigation on the possible application of high frequency STP and the use of skin effect as a valuable tool to determine sub-surface material structure. The images obtained from these scans will then be used to determine whether the basic STP circuit is working. The frequency will then be increased in steps up to a maximum of 1MHz. Higher frequencies are possible as shown in figure 4.11, but the detectable increase in skin depth is getting smaller, because of the a nature of asymtotic curves. These will then be post processed using an image-processing package. The results will then be compared with the expected results as suggested in Figure 4.12 and Figure 4.13. Various types of information can be obtained from the scanned images. A test of the technique is to look for evidence of grain boundaries on a smooth specimen. The grain sizes of the materials are known because

they have previously been measured using SEM images. In addition, the process by which the material is formed produces grain sizes of known size. This information can be used to determine whether we are seeing below the surface of the sample or whether there is some other mechanism at work that prevents us from seeing below the material surface.

If sub-surface imaging is possible then these images can possibly be combined into one image and be used to do STP tomography. The technique of tomography is that several images are combined to form one three-dimensional (3D) image of the object that is scanned. The tomography is not part of this thesis but it would be interesting to know whether it is possible. The use of STP tomography has potentially huge applications in the semiconductor industry. The standard track size in modern high power processors is in the order of 0.1μm. This is well within the scan range for the STP scanner. With the tomography, the end user can then build up a 3D image of (say) a CMOS memory cell, to see how deep the penetration of the doping for the silicon is.

Chapter 5: Pre-amplifier design

5.1 Introduction

The pre-amplifier of a STM system is very important to get the good and clean signal required to run the PI controller to get the topography measure of the surface that is being studied[62]. For the STP implementation an extra constraint is added in that the STM pre-amplifier must also have some bandwidth available in the order of several tenths of kilohertz. The usual STM pre-amplifier bandwidth is less than 100 Hz[1,2,5,9]. This is a result of the trade-off between the very high gain required (10^9) and the bandwidth required, and the noise induced into the signal.

5.2 Noise sources

There are several noise sources in the STM pre-amplifier as is shown in the drawing below[62].

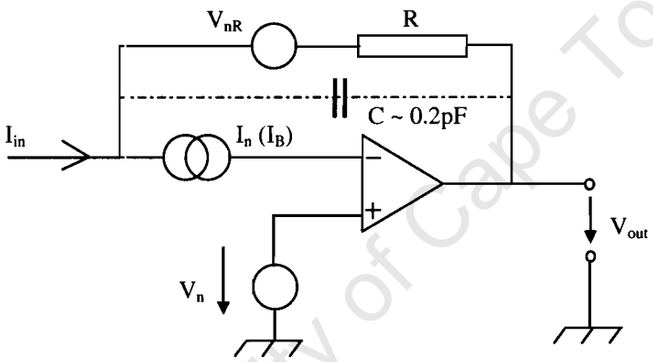

Figure 5.1. Noise sources in the STM pre-amplifier. The basic configuration is that of an IV converter with the parasitic capacitance of 0.2pF. This value is obtained by measuring the response of an actual STM pre-amplifier and then calculated backwards into the amplifier what the capacitance for this configuration will be. I_{in} is the tunneling input current, and V_{out} is the voltage output of the gain stage.

It can be summarized as resistor noise, voltage noise and current noise. The total noise can be written as:

$$\text{Noise} = [\Delta f\,(4kTR + V_N^2\,(I_N R)^2)\,]^{1/2} \qquad [V] \qquad (10)$$

Where Δf is the bandwidth [Hz],

k is Boltzmann's constant [A.s],

T is the temperature in Kelvin,

R is the resistance [Ω],

V_n is voltage noise from the device datasheet [nV/((Hz)^{½})],

I_n is the current noise from the device datasheet [fA/((Hz)^{½})].

It must be noted that the voltage noise is always constant, whereas the current and resistor noise is dependant on the actual resistor value that is used in the amplifier. The resistor noise is also further dependant on temperature.

5.3 Signal to noise ratio

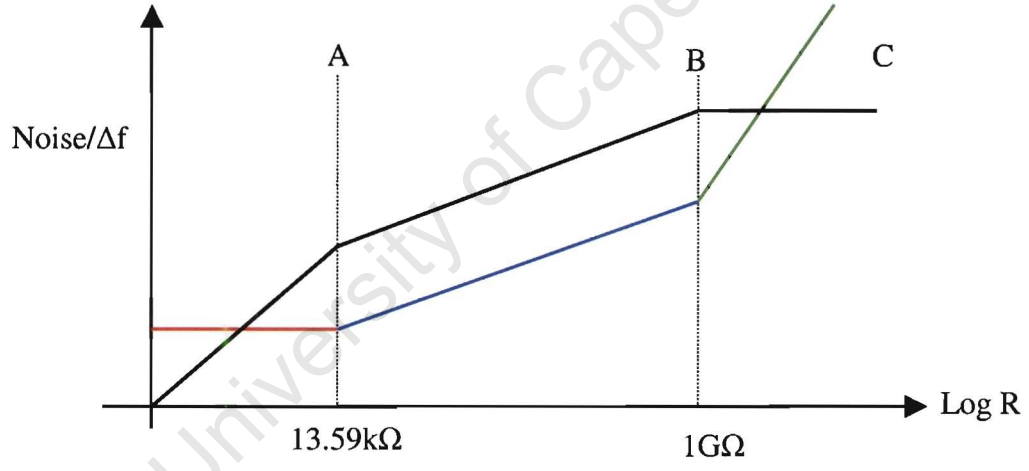

Figure 5.2. This is a graph to show where the respective noise sources are relevant. From the origin to point A, the red line shows only the voltage noise which is constant at all resistor values. At point A the resistor noise starts to play a role and is shown as the blue line section of the graph. It is shown together with the voltage noise (resistor noise + voltage noise). At point C the current noise is becoming significant also and is shown together with the voltage and resistor noise as a green line. The black line represents the total signal to noise ratio at the different resistor values. It can be seen that above point B, the signal to noise ratio drops significantly. The two values that are shown are calculated for this application.

As was mentioned before, the voltage noise is constant for all resistor values. Then it can be calculated for a certain amplifier where the resistor noise is playing a role. For the amplifier that is used in the first stage of the STM amplifier (OPA604), it can be calculated as follows.

At point A the voltage noise is equal to the resistor noise. Therefore:

$$V_N^2 = 4kTR_A \tag{11}$$

Which re-arranges to

$$R_A = V_N^2/(4kT) \tag{12}$$

The same is done where the resistor noise is equal to the current noise and we get

$$R_B = 4kT/(I_n^2) \tag{13}$$

This gives the two resistor values for point A and point B. The values for I_N and V_N are from the datasheet of the OPA604. R_A is equal to 13.59kΩ and R_B is equal to 1GΩ and these two values represent the two values where the resistor noise is more dominant. This also sets the range of the values for the feedback resistor that is used in the first stage of the pre-amplifier. The actual resistor used has a value of 1MΩ, which is between the values of R_A and R_B. According to figure 5.2, the signal to noise ratio below point A would also make for a good solution, but it must be pointed out that the feedback resistor would be too small for this application.

5.4 Amplifier layout

The final amplifier layout can be seen in appendix C. The first gain stage is very fast and has a high gain, but not too high so that some bandwidth is retained on the output of the system. For the STM height controller the next gain stage will limit the bandwidth to roughly 1kHz before it is sampled and used in the Z controller. The STP functions multiply the signals together; hence the high bandwidth signal must still be used for the STP inputs.

5.5 Strategies for reducing the amplifier noise

The amplifier noise can theoretically be reduced by reducing the resistor value, the temperature, and by choosing an amplifier stage that has a lower current and voltage noise rating. For a given amplifier the voltage and current noise is fixed and hence you can only

change the resistor or the environment temperature. Again the resistor value is fixed for a given required gain. The need is to have a high gain in the order of 10^9 so that there is not a possibility in changing the resistance.

The only variable that can change is the temperature of the environment, but this must be done carefully. If it is lowered by say 50 K from room temperature at 294K to 244K by using a cooling unit (i.e. Peltier effect, ammonia cycle etc.) it will reduce the noise by the square root of the temperature reduction. The new problem that arises by doing this is that it generates multiple thermocouples because of the temperature differences between two different metal surfaces (i.e. solder to copper lead). A thermocouple generates a voltage because of the difference in temperature between two metal surfaces. This difference in metals will cause a potential difference and this will influence the measurement of the system as a whole. This thermocouple effect occurs at all temperatures, but for a system at room temperature the system is in equilibrium and can easily be compensated for. If the resistor of the pre-amplifier is cooled down, the complete set of electronics must be cooled down. Since the STM scanner is to be used in air and at room temperature, the cooling of the pre-amplifier to reduce the noise will complicate the system, and push up the overall cost of the system. One of the aims of this STM is to keep the cost to the minimum. It is therefore not used in this STM.

5.6 Conclusion

Although the noise level can be reduced by reducing the temperature of the system, the cost of the complete solution must also be kept to a minimum. This leaves us with a low noise, low leakage current, pre-amplifier that is suitable for wide bandwidth and high gain applications like STP measurements. The amplifier frequency response will be shown in a later chapter along with the results of the STP scans to show that this project produced a suitable pre-amplifier for this specific application.

Chapter 6: A redesigned embedded data acquisition system

6.1 Introduction

This chapter describes two new iterations of the data acquisition system. The project started with the data acquisition system as it was taken from the previous study[14] and tried to improve the software as a first step to learn more about the requirements of a new implementation. The new system that was proposed in the previous study was then implemented and tested. A picture of the communications interface between the system and the PC can be seen in figure 6.1. The X and Y directional controllers were also split into 2 separate parts and can be seen in figure 6.2.

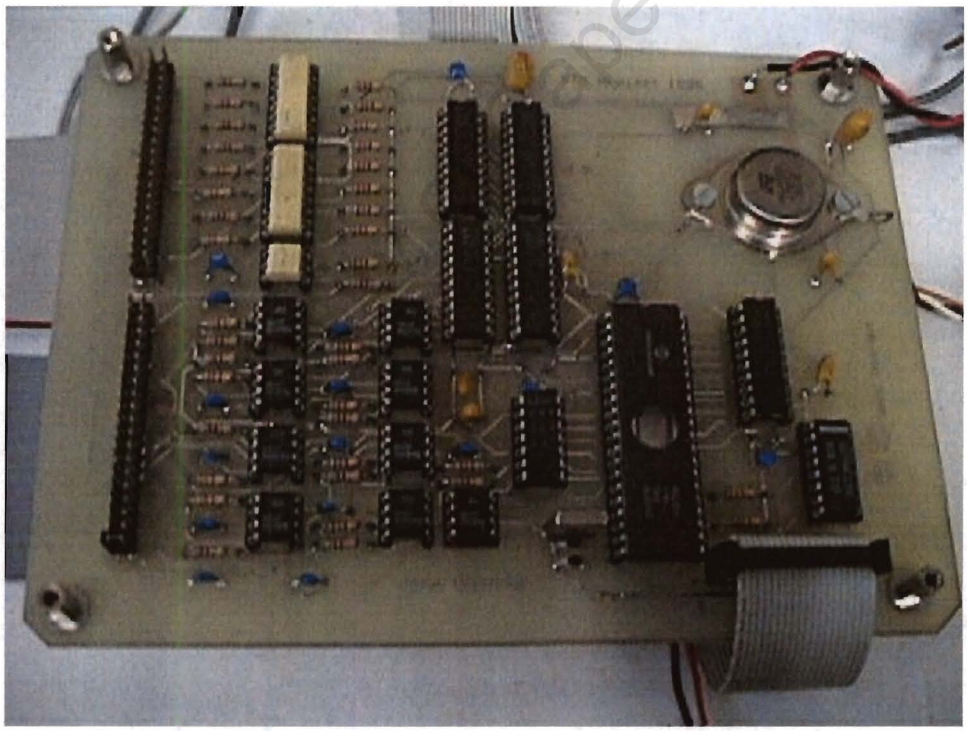

Figure 6.1 Photograph of the parallel interface to the PC. This board is also the master in the system of four microcontrollers. The two parallel interface links to the PC are visible on the left. The parallel cable that is visible on the front is for signalling to the other components of the system and for the serial ports.

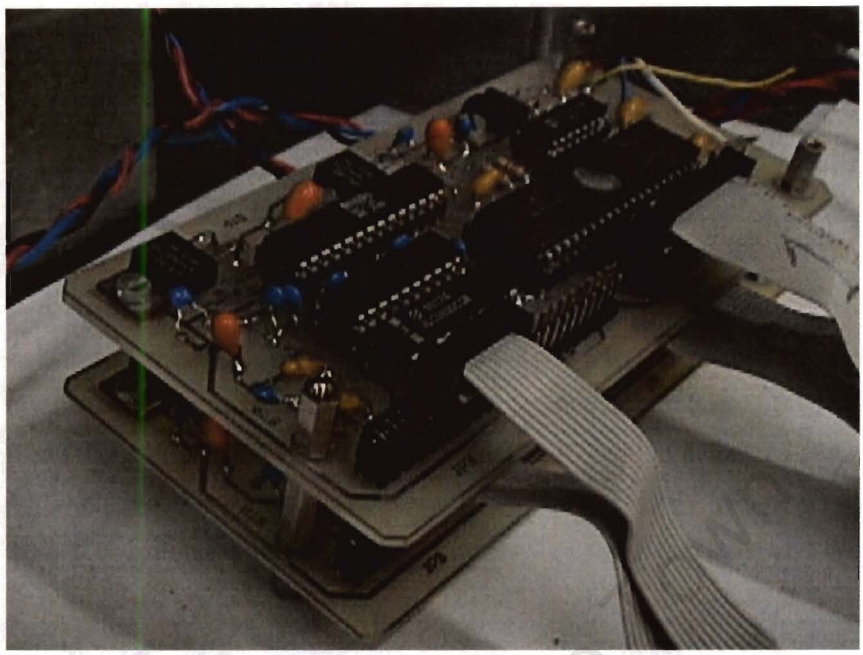

Figure 6.2 Photograph of the STP boards where they are connected together in their stack. Each board has a 16-bit DAC and two 8-bit ADCs. All the extra signals like the counter, PWM and capture signal pins are extended onto the headers.

This system was then developed and tested along with Visual C++ code and is explained in this chapter. The Visual C++ code was the same as in the previous study except that the STP data was now also stored. However some problems proved difficult to solve with the communications interface to the PC and the PC program. The reasons for this will be explained later in this chapter. This prompted the redevelopment of the PC software and the communications interface to the PC. The parallel port was changed for a serial port and the PC software was rewritten under Labview. A picture of the new serial based communications interface can be seen in figure 6.3. The rest of the system stayed the same, no changes were made in the X, Y or Z controllers to accommodate the new serial based communications interface.

This chapter will first describe the parallel-based communications interface, and the associated PC software, then followed by the X and Y directional controllers. This will then be followed by the serial based communications interface and the reasons for changing it.

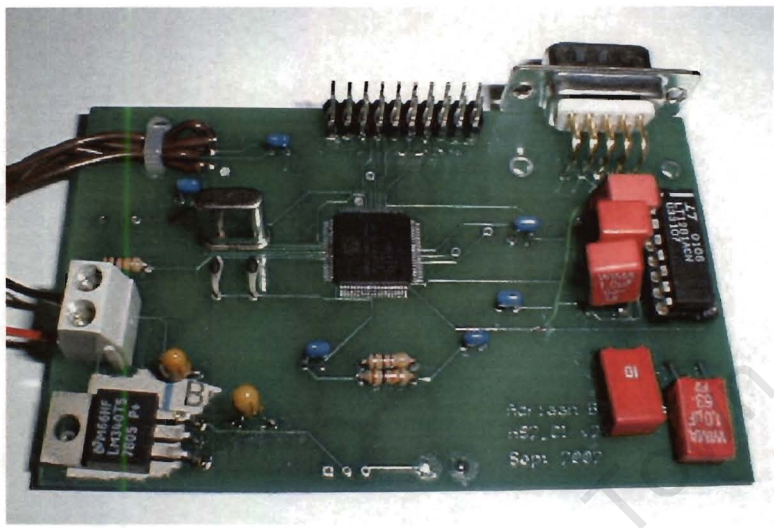

Figure 6.3 A photograph of the PIC18C8720 based system that communicates to the PC via RS-232. The processor is seen in the middle with the RS-232 chip and the connector visible on the right side. The connector on the middle top is connecting the X, Y and Z controllers to the communications unit. The wires on the top left side are the programming interface for the flash memory of the processor.

6.2 Parallel-based communications interface

The new parallel communications interface was designed to act as the interface and control board between the PC and the rest of the embedded system. During the author's previous iteration of the electronics[14], it was suggested that the system be split up into several more microcontrollers. It would theoretically simplify the system by giving smaller tasks to each microcontroller. In this case, the XY controller would have been split up into a communications interface to the PC, an X direction controller, and a Y direction controller. The Z controller would then stay unchanged on it's own microcontroller, as in the previous iteration[14].

The parallel based interface uses many features that were found on the previous iteration of the interface board. The previous board was called the *XY controller* and did the X and Y directional control for the STM also. The interface to the PC consisted of an optically isolated parallel link to a PC–14 card inside the PC. The new *high-speed communications interface* (HI_CI) also uses this method of interfacing to the PC. The reason for this is that a parallel

interface can transfer more data, and the fact that a custom written device driver was available to do the data handling for the system. The device driver was previously written by Bernard Kuc for the author's MTech research at the Cape Technikon [14]

The device driver usually sits between the hardware and the operating system, thus enabling it to operate extremely quickly because it can command more of the CPU time (of the PC) than the operating system. It does not have to request execution time from the operating system (as an application that sits on top of the operating system, has to do). A feature of the device driver that makes it very useful is the custom read sequence that was programmed into the system. This method uses the device driver to read a thousand bytes of information and then passes this information as an array to the application program level of the operating system. Using this method very high transfer speeds can be obtained (in the order of 40 kbytes per second). An additional description was given earlier in this thesis in Chapter 3.

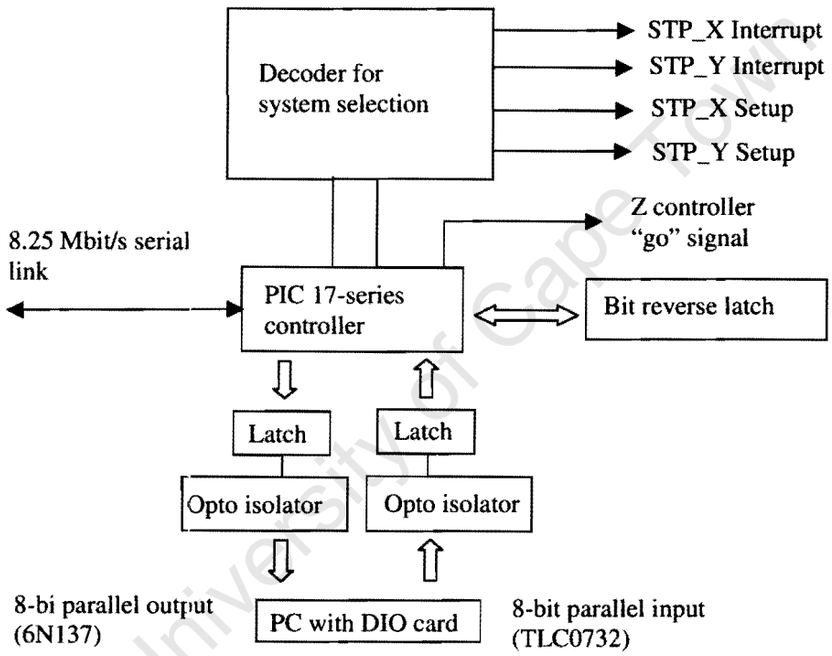

Figure 6.4 A drawing of the high-speed communications interface, showing the signal flow paths and the signals that is used to control the rest of the system. The high-speed serial bus and the bit reverse latch can also be seen along with the opto-isolated ports to and from the PC.

Currently the high-speed communications interface (HS_CI) consists of the parallel port interface, the synchronous serial interface and a set of latches that is used for data manipulation. Each of these will be discussed below along with a section on the software interface that is required.

6.2.1 Parallel interface to the PC.

The new configuration for the parallel interface uses the 6N137 digital opto-coupler to interface to the PC. This opto-coupler can handle transfer speed up to 10 Mbits per second. The previous interface could not handle the throughput because the 4N25 devices that were used deformed the signals, causing errors and incorrect data to appear on the PC. The reason for using opto-couplers is the noise isolation that is required from the PC. Tapson[13] proved that the PC ground lines (digital and analogue) are the source of large amounts of noise in STM measurements. Up to 100 mV of noise can be measured, corresponding to a least 3 bits in a typical 8-bit ADC range. By separating the ground lines, and using a separate power supply to power the measurement electronics, a very low level of noise can be observed. Only the one side of the interface uses these fast opto-couplers. The download side from the PC to the interface still uses the slow 4N25 and Toshiba TLC0732 because the setup information from the PC does not require expensive and fast components.

During a scan a sustained rate of about 12 kbytes per second is achieved, which is fast enough for the existing system that scans at a rate of 3 kHz in the lateral direction. The data that is sent to the PC is bit reversed because the Z controller uses the PCM1702 DAC that wants it's data transmitted MSB first. The solution to sending the bit-reversed data to the PC is to wire the output port in a bit reversed pattern, and thus reversing the bit reversed data. The PC then gets data that is formatted correctly. This has the effect of not adding any processing requirements to the system. The schematic diagram for the system is shown in appendix A.

6.2.2 Common serial bus

The four microcontrollers communicate on a common synchronous serial bus with each other. It works on a master slave protocol that requires each processor to grab the serial bus master mode when it is its turn to transmit. The process starts by placing all the processors in slave mode (with receive activated). The microcontrollers all boot up after power up, but only the

high speed communications interface will be in a master mode with its transmit activated. The process as it happens further on is explained below by means of flowcharts.

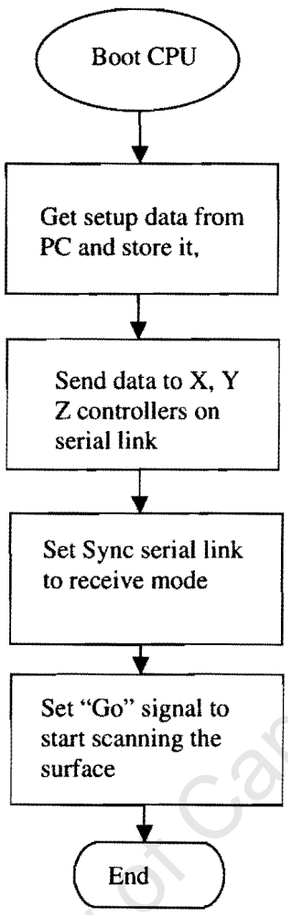

Figure 6.5 Flowchart to show the program flow before a scan is started. The setup data is received from the PC and then distributed to the various parts of the system to configure them.

Now here is where a rather big problem comes into play. The previous four bytes were generated by the Z controller and the fifth and final byte was generated by the STP controller. The four bytes from the Z controller are sent in a bit reversed (MSB first) format. This is easily corrected by wiring the parallel output port in a bit reversed format (see appendix A). If the fifth byte is bit reversed in the parallel port it will be difficult to correct it once it is in the PC. The first four bytes are however correct after it passed through the parallel port. To reverse the fifth byte before it is reversed again in the parallel port, a latch-based system was developed.

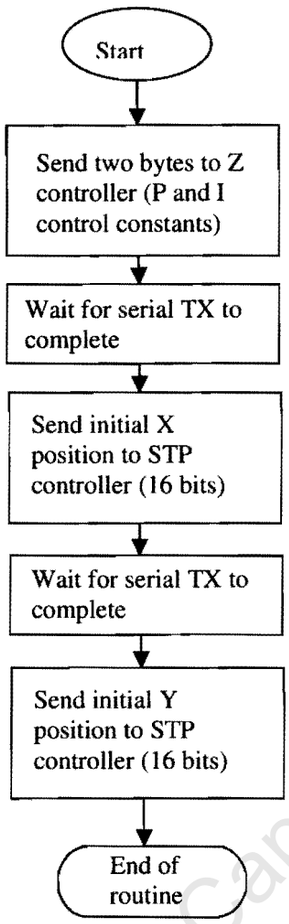

Figure 6.6 Flowchart of the setup information being distributed to the various subsystems. It can be seen that the basic process is quite simple; the only requirement is to check that the serial port does not overflow. To prevent this, a small time delay is added after each data transmission.

The result that is read from the double latch is the bit reversed 8-bit ADC STP value. This actual code implementation is very fast and efficient and takes only seven lines of assembler code to drive the hardware. See Appendix A for the schematic diagram and Appendix F for the assembler code.

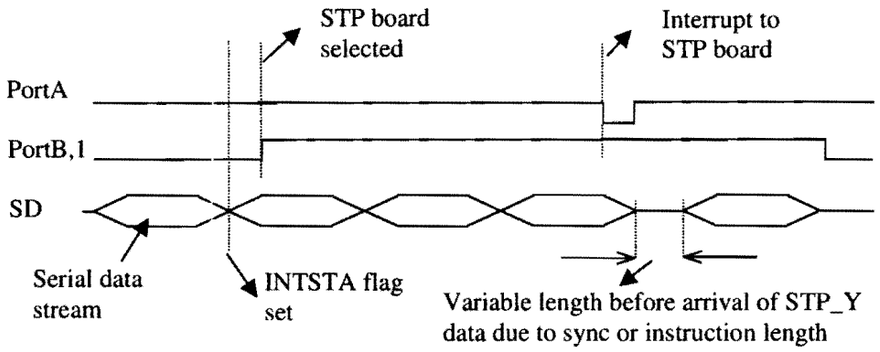

Figure 6.7 A timing diagram of the five-byte serial stream that is transmitted at 60 kHz. Each data byte is transmitted MSB first except the last one which has to be bit reversed first. The time of the interrupt signal being generated and the response of the system can be seen along with the signals that the system generate to force the STP controller to transmit the STP Y directional information.

6.3 STP measurement board

The measurement of the analogue parameters such as the STP analogue detector signal is done by the STP boards along with the raster pattern generation. Each STP measurement board has two eight-bit ADCs, a 16-bit DAC and a PIC17c4x microcontroller onboard. The board was designed to be very compact and to be reusable. This means that all the required port pin connections were brought out to headers. In the following sub sections, the complete working of the STP measurement board will be discussed.

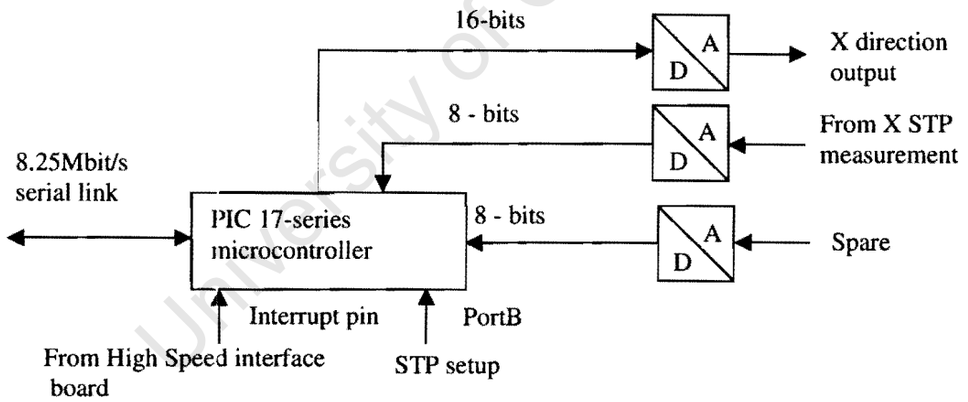

Figure 6.8 Diagram of the X directional STP board with the signalling and data acquisition pathways shown. The signalling wire to the interrupt pin forces an immediate transfer of STP data onto the serial bus, the setup wire that connects to PortB tells the system when it must receive setup information, and also acts as a "Go" signal.

6.3.1 Accessing the serial port

The serial data transmission is requested by the high-speed communications interface by toggling various pins on the STP microcontroller. In the case of the STP measurement data, the interrupt pin on PORTA is toggled to indicate to the STP controller that the communications interface is requesting the data for the second STP channel. The first STP channel is on the Z controller and that data was transmitted as the fourth byte in the serial stream.

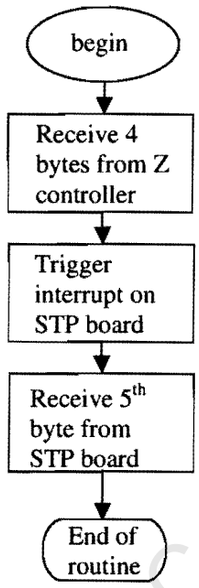

Figure 6.9 Flowchart showing the sequence of events to get the 5th byte in the serial stream from the STP controller. The communications interface will send the trigger signal to the STP board to get the data byte.

6.3.2 Generating the raster pattern

The raster pattern is generated following a request from the HS_CI. This request was implemented by using one of the port pins on PORTB and generating a peripheral interrupt on the port pin changed feature of the microcontroller.

There are two STP boards and both have the same software on them. The way that they are different is very small. Each of the two STP boards uses one of the port pins to determine whether it is the X or Y STP board. During the setup four bytes are loaded from the HS_CI,

and depending whether pin 5 is tied high or low, they will determine which of the two STP boards will react to the setup information that is transmitted on the common serial link. This means that both STP boards use the same pins to trigger a DAC advance, but the HS_CI uses separate cable connections to trigger only the required system. In this way irregularly shaped scan patterns can be generated.

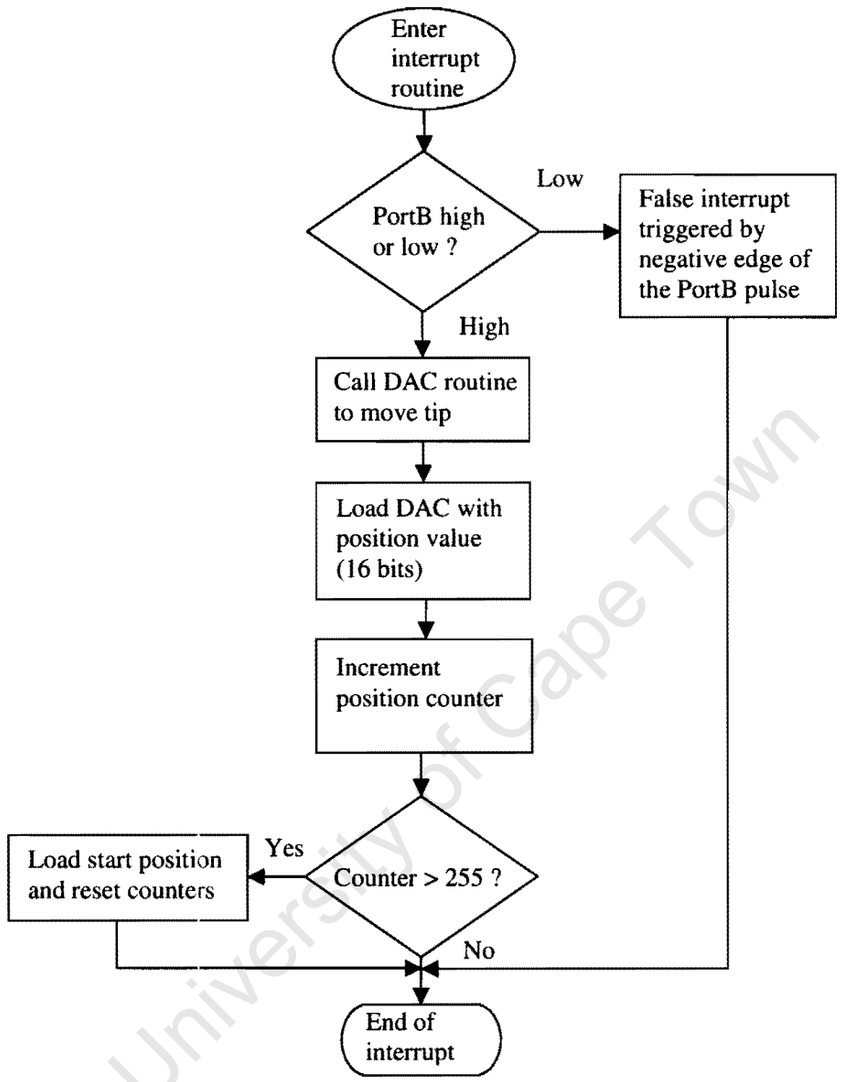

Figure 6.10 Flowchart of the interrupt routine that is triggered by a change on port pin feature of the microcontroller. The interrupt gets triggered by both the positive and negative edges of a pulse. This is tested for, and on a positive edge, the DAC routine is called. Once the end of the scan line is reached, the counter overflow will cause the counters and DAC position to be reloaded. The sequence of events are the same for X and Y controllers, but is controlled separately by the communications interface.

6.4 Scheduling of the various tasks

The scheduling of the various tasks that have to be performed can make a huge difference in the operation of the microcontrollers, and on how fast they perform the tasks at hand. In order to understand this, it is vital to break the tasks into three separate sections; those tasks that are time critical and that must be performed every 60us, those that are normal priority and must be performed outside of an interrupt, and those that are of low priority and can be done when no other task is executing. The time critical tasks are normally added in an interrupt service routine where they can be controlled by a timer interrupt or other regular interrupt from (say) a timer. The normal tasks are executed between interrupts, and the low priority tasks are just implemented as house keeping tasks. These are sneaked in between normal tasks if the normal tasks are waiting for interrupts or other external signals to be triggered. This can be done because it will take a few microseconds before the PC will assert the pin to the state that the instruction will be testing for.

In the previous iteration of the embedded system[14] the downloads took 3 bytes per download to the PC, but in the new system it has to transmit 5 bytes to the PC and still keep the same download speed. This was done by scheduling the various tasks so that instead of incrementing the DAC, then waiting for 10 readings to arrive, and then transferring it to the PC, the signalling was modified to be of a different priority level. The DAC was placed at the start location and then the scan was started. After the minimum required number of data sets was received, the last data set was transferred to temporary storage and the DAC was signalled to move the tip. While the tip was moving to a new position, the five bytes were downloaded to the PC. By the time this download was finished a brief check was done to determine that a set number of data sets had arrived as minimum before the PC transfer is called again. In this way the data transfer rate was maintained at 12kbytes/s. This means the 486 PC was now the bottleneck in the system, and not the embedded system because the microcontrollers could work much faster than the PC with Windows NT 4 running.

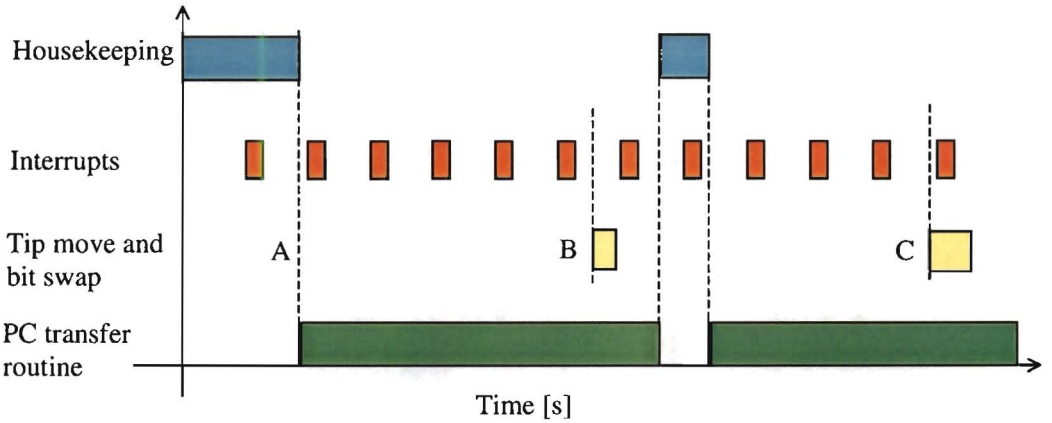

Figure 6.11 Gant chart showing the execution times of the various tasks at hand that have to be executed. The four main activities for the high-speed communications interface are show in this diagram. Green, yellow and red blocks indicate the program sitting in a subroutine. After the processor boots up, the tip is positioned, the scan is started and the first serial data is received; right after this, the data transmission to the PC is started. At point B, the fifth byte that will be sent to the PC, is bit swapped and the raster pattern is incremented. After the download to the PC is completed, various housekeeping tasks are done and the process is repeated. At point C, it must be noted that the serial port interrupted the working of the bit swap, resulting in that section of code executing longer.

There are other ways of designing the code, but this method was the easiest to implement. Other methods could be a time slicing system that gives equal amounts of processing to different tasks, or even rearranging the tasks at hand to save a complete scan line in memory before downloading it to the PC. Time slicing would create more problems because not all the tasks at hand are of equal length, and the synchronising would have posed more problems. The scheduling of the tasks also takes up lots of processing power, which means that a more powerful processor has to be used, hence increasing the system cost. Another method is to save a complete scan line of 5 bytes for each of 256 data points, which is equal to 1.25 Kbytes of data, in external memory. This has to be done using a table write operation in the PIC series, which takes some time. It also means the scan has to be halted at the end of each line to do a transfer to the PC so it is not very efficient.

It is better to transfer each data point immediately to the PC because that has the effect of using less CPU overhead, less memory, and the final program is relatively simple.

6.5 Serial interface to the PC

The PC interface was given an extra iteration and the 486 based PC system was removed, and replaced with a 1GHz Pentium 3 after a gap of several months, and the high-speed communications interface was removed also. In its place was put a serial link that runs at 115.2kbits/s in a RS-232 protocol. This is the maximum speed for this protocol. The reason for the change was that the 486-system was too slow, and could not run a modern development environment like Labview[44]. The parallel data ports using a PC-14 card were designed to get high data throughput on this slow PC, which worked well but in the intervening months, the average PC became very fast and hence new and better options became available. The 12kbyte/s of the parallel system is equal to 96kbits/s, hence the serial and parallel based systems are of approximately equal speed.

The new interface board uses the exact same software that the previous iteration of the high-speed communications interfaced used, except the data is not transferred in parallel but in serial. The actual assembler code is the same except for a few register name changes. The processor that is used for this is the PIC18c8720. The PIC17 series devices control the X, Y and Z directional scan movements as before. The microprocessor board now links to the PC via RS-232, and on the PC there is a Labview interface that controls the serial port reading and writing functions. At the speed of 115.2kbits/s the serial link is fast enough to handle the data transfer requirements of the STM system with the STP functions. The PIC18c8720 has several serial ports; the first is now used as an RS-232 port to the PC, and the second is configured as a synchronous serial port running at 8.25Mbit/s to communicate to the X, Y and Z movement controllers.

The serial interface is also renders the bit-swap function that was implemented in hardware obsolete. This is now done in software under Labview. The Labview source code is provided in appendix F. A picture of the serial communications interface is provided in figure 6.3.

6.6.1 New PC software

New PC software was developed to aid in the pre-processing of the STM and STP data. This software was developed in Visual C++ and was made available as three separate programs. Each program helps with the splitting of the scan data file into, STM data, STP X directional

data and STP Y directional data. The new data file contains only the required data, is then saved with an appropriate extension name to indicate what type of data it contains. Each program was also given the ability to display the data in a line type display. This helped in deciding which data will be post processed on a Sun workstation. Only data files that looked promising were processed, to save time, but when the user has more time available, it would be advisable to process all data to see if there is something interesting in the not immediately interesting data files.

The STM software data handling was also changed to store the STP data correctly. The STM data and STP data now alternate in the data archive. The display routine was also optimised to make the display more appealing and understandable.

6.6.2 Labview based PC software

After the experience gained in the intervening time, the Visual C++ interface was dropped in favour of a Labview[44] program. The Labview environment gave more options for designing attractive graphics, and for giving the imaged surfaces immediately without the need for post processing on a workstation like such needed for the Visual C++ interface. The Labview environment is also runs on a 1GHz Pentium Laptop, and gives excellent performance. The added feature of Labview is that the program flow of the system can be seen because the programming environment is based on block diagrams. This makes the understanding of the program much easier, and anybody with a basic understanding can read the program and immediately understand it.

The older versions of Labview were slow and Visual C++ had the edge over Labview when it came to speed of execution. This was especially true for the 486 based PC that most of the previous work[14] and a large part of the current work was done with. Labview version 6 is much faster because National Instruments[44] has optimized it. If used on a 1GHz Pentium 3 machine, the speed advantage of Visual C++ for this application is lost. The emphasis is shifted to ease of programming and programming time. In both of these cases, Labview is much better than Visual C++. The current STP Labview interface was programmed in one day and one afternoon, and includes the graphic displays, the serial port routines, the arrays that stored the data, and the routines to save the data. The Visual C++ interface in comparison took over 3 months to get working for this project.

6.7 Conclusion

A new data acquisition system was designed to replace the existing system that was designed as a second iteration to the system that was designed by Tapson[13]. This third iteration of the electronics delivered a system that could still be modular, but had the advantage of being fast. The results that were obtained using this new configuration are presented in a later chapter.

Chapter 7: Results

7.1 Introduction

The results of this project were mixed. The parts of the project that were successful were the high frequency wide bandwidth pre-amplifier, the design of a high frequency detector circuit for STP, the optimisation of the Z controller software, the design of a data acquisition and control system for STP, and the study of the effects of current penetration into the material surface. The wide band, high gain pre-amplifier, and skin effects were described in Chapters 4 and 5. The assembler code for the optimised Z controller is available in Appendix F. The parts that were less successful were the choices of configuration of the data acquisition system. This is however also a useful result in another sense because it is now known where the decision boundary is between a single microcontroller and several microcontrollers that are networked together on a serial bus, and a DSP solution lies. This will be discussed later in this chapter.

7.2 Embedded data acquisition system

The design of the data acquisition system was successful in that it provided a system that was functional, but it did not make the final grade of being able to scan in the XY plane at frequencies of 3 kHz. The 3 kHz design limit was set by the first resonant frequency of the scanner tube and its assembly. The resonant curve plot can be seen in Figure 3.5. The final lateral scan frequency was only 1.953 kHz at best. The average scan frequency was 1.843 kHz and the slowest that was recorded was 1.400 kHz. The microcontrollers were fast enough but the 486-based PC that was running Windows NT was slowing the system down. Changing the PC for a much faster Pentium 3 based system solved this problem. The four-processor microcontroller system did make the system extremely modular, paving the way for the addition of a DSP processor in the system.

The second iteration of the high-speed communications interface obtained the same results with the RS-232 port. The system worked easily up to the limit of control at 3 kHz, and since the PIC18 is not using a bit-swap and also not inverting the signals to compensate for the inverting action of the opto-couplers, it is using less code and is thus even faster.

During the final qualifying test of the STM system, it was found that the piezo tube would go into an unexplained resonance for no apparent reason, this was because of too much gain for the PI controller. It is thus also important to get a feel for what the system does. The gain of the controller would depend on the type of material that is used for a sample.

Previously Tapson[13] achieved a Z sampling update rate of 55kHz and the author managed to achieve an update rate of 42 kHz during a previous study[14]. During this study, the Z controller was operated for the first time at an update rate of at least 60kHz. The reason for the 60 kHz bandwidth was explained in Chapter 3.

It must be note that there is a difference between the bandwidth of control and the sampling bandwidth. The sampling bandwidth is the rate at which the ADC is sampled to get new information into the processor. The bandwidth of control is the rate at which the DAC is updated to move the tip to a new position in the Z direction and is defined as that bandwidth at which the response of the closed-loop control system should be below –3dB. This author always used a sample and update scheme, where the control bandwidth and sample bandwidth was essentially the same[14]. Tapson used a sampling bandwidth of 55kHz, but used a much reduced control bandwidth (3kHz) and also scanned much more slowly[13].

What is known about the resonant response in the Z direction of the scanner is that the first resonant peak is normally very much higher than the first resonant peak in the XY direction that is shown in Figure 3.5. What appears to be happening is that there is a first resonant peak at say 70kHz. The scan at a control bandwidth of 60 kHz is becoming unstable, and is just unstable enough to prevent a good tunneling junction from forming.

The solution to this problem was to bring the scan update frequency (bandwidth of control) right down and use a slow controller (reduced gain) at the same time. This means the controller will only make small changes in the Z direction. The controller code was modified so that instead of taking a current reading and acting on it 60000 times a second, lots of readings were taken, but it was only updated 3000 times a second. The sampling rate was at 60kHz and the control bandwidth was set to 3kHz. This left lots of potential processing capacity on the Z controller because it had only had to access the 20-bit serial DAC 3000 times a second and not 60000 times. It was found that by doing it in this way, that the scan

rate in the XY direction could be increased to the limit of 3 kHz because it also freed up the high-speed communications interface. The lower Z control frequency meant that the amount of data that was processed, was lower by a factor of 20 and that the high speed communications interface had more than enough processing power to accomplish the tasks at hand. The 3 kHz lateral scan speed is the highest lateral scan speed that can be achieved and is an important result. It is not possible to scan faster in the XY direction because of a resonance peak at 10kHz. See Figure 3.5. It proves that the lateral control algorithm is working correctly and in this way is also giving the shortest scan time ever for this instrument for a 256 x 256 data point image.

The reduction of the Z control bandwidth is a quick fix to get it the system running and an attempt at getting good noise free images. A 3 kHz control bandwidth is still very good and is in line with what Tapson used previously[13]. It is not known what the noise contribution of running the update rate to close to the first resonant peak in the Z direction is. For that reason, it was a good choice to rather get the update rate as far as possible from the resonant peak in the Z direction. Tapson[13] and the author in the previous studies did not discover this problem in the Z direction so it is not know if some of the images that were obtained previously at a control bandwidth of 42 kHz[14] were contaminated by resonant noise because of the high control bandwidth that was used.

7.2.1 STP pre-amplifier

Initial tests on the pre-amplifier showed that the preamplifier design by Demming *et al*[58] is not a wide bandwidth application. That application was designed for use with an STM only. The circuit as was suggested, had to be modified to get the required 50kHz bandwidth for STP. The new circuit diagram is given in appendix C. The phase and magnitude plots that are shown below are presented to show that the phase is essentially flat over the frequency range that is of interest. This is very important when we look at Equation 4.6, where the phase and frequency difference has to be more or less zero to enable the reading of STP data.

The magnitude on the other hand did show a strange dip at 100kHz. It looks like a band stop filter is active in that region. This could be because of the combination of leads and cables that are used to interconnect the various parts of the system. This was tested by only measuring at the output of the pre-amplifier and it was found that there was no band stop filter

action present without the interconnecting cabling, hence in the complete system this cabling must be used, and is therefore taken into account. A Bode plot of the response is shown below. It can also be seen that the phase varies slightly, but never by more than about +27° or –9°. The magnitude of the signals that were read was normalised to zero dB, because a manual gain adjust can be done using the final gain stage in the STP detector to obtain the same effect. Before the test was conducted, a test signal was used to try to set a gain of unity from the tunneling junction to the input of the ADC.

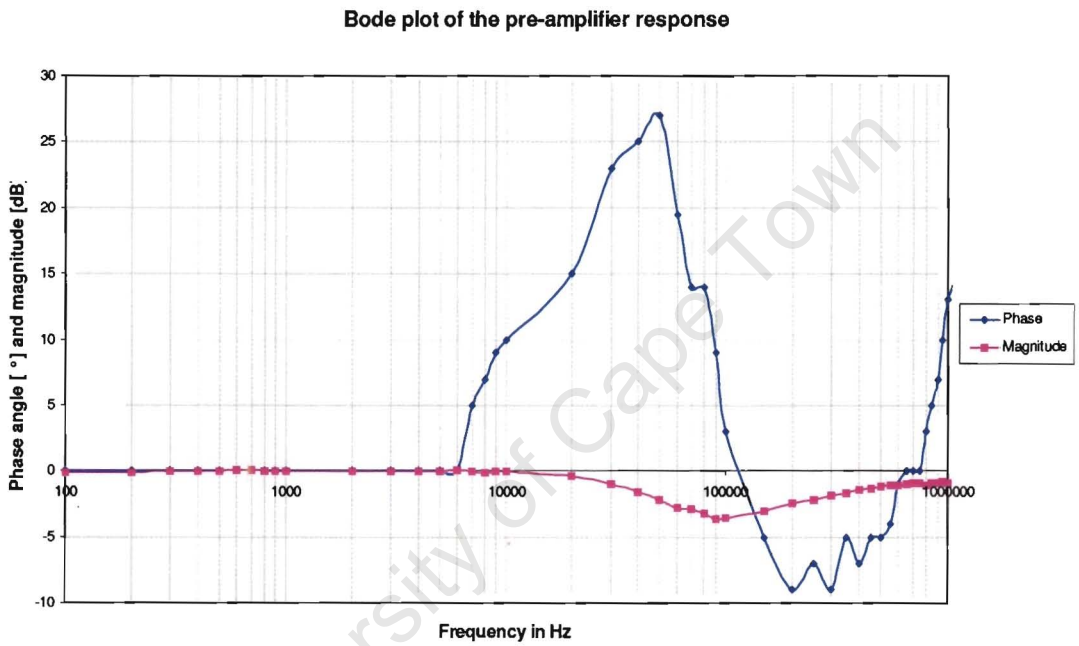

Figure 7.1 Bode plot of the preamplifier response. The response was measured from the input at the tunneling tip up to the input of the ADC that samples the pre-amp output. It can be seen that the frequency response is flat up to 10kHz, but takes a dip at 100 kHz down to about –3.6 dB. The phase also varies at the same time, but not by more than about 27°. This is discussed elsewhere in this chapter.

The signal level is not reduced by much, the –3.6dB drop can be compensated for by increasing the gain of the op-amps that are used on the output of the final stage if measurements are done around 100 kHz.

7.2.2 STM results

The Z controller was essentially the same device that was used for the author's MTech project[13, 25, 60]. Three new images are shown below. These scans prove that the Z controller,

the high-speed communications and the pre-amplifier are working. The incrementing raster generators on the STP boards are also working. It is important that the wide-bandwidth pre-amplifier that was developed for STP applications is working for purely STM applications also. The only items that need to be proved operational still are the actual STP detectors and the STP sampling circuits.

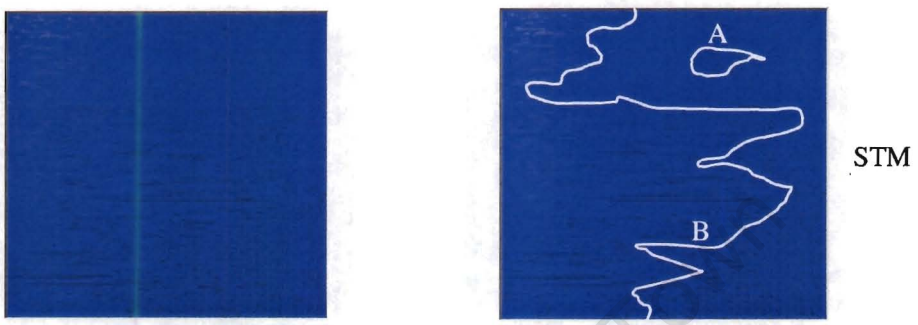

Figure 7.2 An STM image. On the left side is the original image and on the right side some areas have been marked to highlight some basic features on this gold surface. The area denoted by "A" shows an example of an area filled with contamination (dirt). The line marked "B", shows the approximate location of a step edge on the gold surface. The image is 256x256 datapoints and has a size of 1.2 x 1.2 μm^2

Figure 7.3 An STM image. On the left is the original image and on the right is the same image but with areas marked in white for clarity. Line "A" represents a step edge on the surface of the gold sample. The surface above line "A" could not be resolved clearly. This means there are possibly mobile molecules on the surface that are being pushed around by the STM tip. Again the image is 256x256 datapoints and has a size of 1.2 x 1.2 μm^2

7.2.3 STP results based on the 50kHz detector

The images that are presented here are from a single scan of the gold plated sample surface. The sample was polished to obtain a flat appearance for initial trials of the STM instrument.

In Figure 7.4 the X and Y channels of the STP detector output can be seen. The two images are slightly different due to the alignment of the crystal structure of the gold sample in the X and Y directions. The associated STM image is also shown.

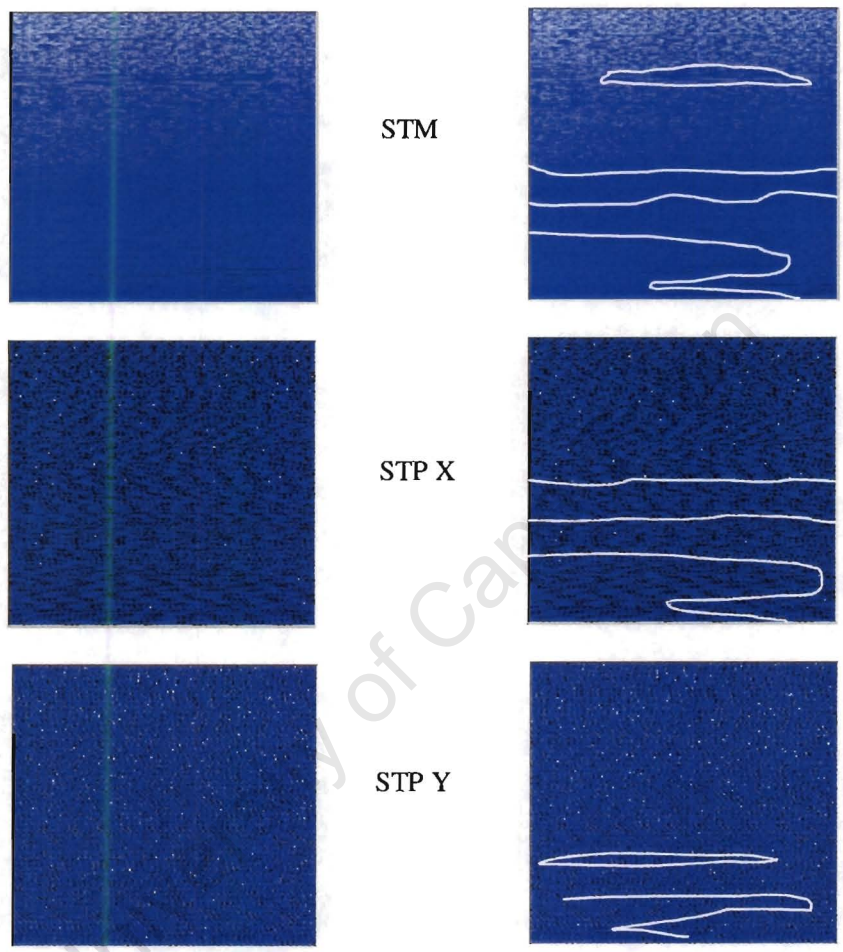

Figure 7.4 A STP image set, from top to bottom are the STM scan, the STP X direction and the STP Y direction scans. On the right side the same images are shown with added lines to highlight some features. The STM image shows three features, an oval area on the top, a groove-like feature in the middle and an area at the bottom. The STP X direction image shows the groove structure and the area at the bottom, but not the oval shaped structure at the top. This could be because this structure is not in the surface but has something loose lying on top. The STP Y directional image shows little information, indicating that the subsurface structures are orientated in such a way as to not cause a potential difference. Image size is 1.2 x 1.2 μm^2.

7.3 Conclusions

The Z controller induced a resonant frequency response in the piezo voltage at 60kHz due to the 60kHz control bandwidth that was used. A lower control bandwidth is better because it

prevents high resonant frequencies from being produced in the piezo tube, while still keeping the 60kHz sampling bandwidth.

A bode plot was done to determine the response of the pre-amplifier circuit that is used for STP and STM. The pre-amplifier must have a flat response in both phase and frequency to make sure that Equation 4.6 is valid. This design was achieved and several STM images were obtained with this wide band STM pre-amplifier. Normally a STM pre-amplifier has a bandwidth of several Hz[1, 2, 13] at most, but the one used in the new design has a bandwidth of 100kHz.

A continuation project can now be performed to obtain new STP data on various samples like Carbon and Platinum. One of the first tests that must be done is to determine whether we are getting valid STP data. This is done by obtaining STP data at different magnifications to see if the size of the features that are observed are changing. A test that is similar to this is to rotate the sample through 90° to check that the features in the STP images also rotate. This will form part of the future work.

The electronics is working satisfactory as can be seen from the STM scans and from the STP data that is presented. In conclusion, it can be said that the project provided a system that can control the scanning of a STM with STP capabilities. The 50kHz STP detector is working and was used to produce a set of STP images using the new data acquisition system. The 1 MHz detector was only bench tested to confirm that the PCB layout is correct and that the expected signals are appearing on the outputs.

In conclusion, a summary of all the work that was done for this dissertation is presented.

- The tip assembly was removed from the STM scanner and a new housing was constructed from a ceramic material into which the tip could be placed. A photograph of the new tip holder is shown in Figure 7.5. It can be compared to an earlier photo of the tip in the scan head in Figure 3.3. This also had the additional objective of checking that the tip assembly was still in good order and clean. It must be clean of any contaminates, even the salty deposits in a finger print will act as a conductive path for current away from the intended path towards the current pre-amplifier.

Before any scans were conducted, cleaning alcohol was used to clean the conductive pathways on the pre-amplifier and on the output from the Z output DAC.

Figure 7.5 The new ceramic tip holder can be seen in this photograph. This can be compared to Figure 3.3 where the tip holder construction is still different.

- A new pre-amplifier was constructed that has a very low input leakage current[58]. This new preamplifier uses two op-amps, the first is a very expensive OPA604 and the second is a LM6361. The choice for the second op-amp is not critical. The OPA604 has an input leakage current of about 1pA, which is several orders of magnitude lower that the 0.1 to 1nA current that the pre-amplifier is trying to amplify. A surface mount PCB was designed for the new pre-amplifier. The surface mount PCB is also smaller than a through-hole plated PCB, resulting in smaller stray capacitance values. This helped in getting a flat frequency response and very little phase shift. This can be seen in the Bode plot in Figure 7.2. A photo of the scan head with the improved pre-amplifier can be seen below.

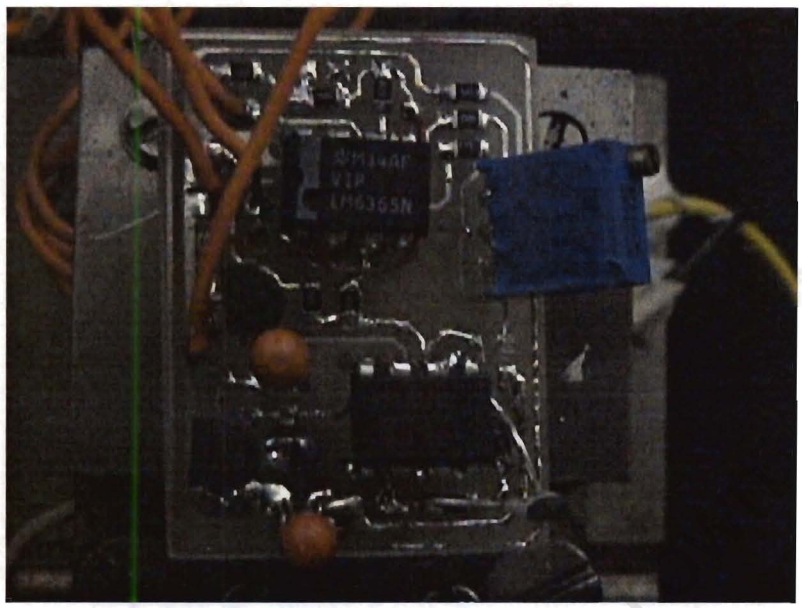

Figure 7.6 Photograph of the new pre-amplifier as it rests on the scan head. The input to the amplifier is near the bottom of the image on pin 2 of the OPA604 IC. To reduce noise the PCB was designed to be as small as possible.

- The Z controller code was also optimised for execution speed. During the final stages of the previous study[14], a timing error was discovered on the XY controller. The DAC712 needed a longer write pulse than expected to clock the information into the DAC registers. The only way to achieve a quick fix was to lower the clock speed of the XY controller. This gave the required timing, but the synchronous serial port running to the Z controller could not connect at the high speed any more. By lowering the Z controller clock speed to 20MHz, to match the XY controller clock speed, the serial port could still be run at the maximum speed of 5Mbit/s. The baud rate generator is dependent on the clock frequency.

The Z control loop now ran at 42kHz, which is below the required 60kHz. Further more, the second ADC0820 was also now used on the Z controller board to do STP measurements. The STP data was coded into the fourth byte that was transmitted in the serial stream to the XY controller. Previously the fourth byte was just a dummy byte, hence the data stream was still the same length. The extra code length reduced the loop execution time down to 38kHz. The optimisation of the control loop involved removing all of the call, return and goto instructions from the program. The code was thus turned

into a straight-line version. A copy of the code is given in appendix F. The new execution speed was increased to 46kHz at a crystal frequency of 20MHz.

In the new four-processor system, where the DAC712 ICs form part of the STP controllers, the timing problem is no longer an issue. This means that the clock frequency of the entire system can be raised to 33MHz again. At 33MHz the Z control loop code executed at 67kHz, which is faster than the minimum requirement of 60kHz. A delay loop was added in the Z control loop code to bring the loop execution time down to 60kHz again.

- Theoretical calculations were done and presented in the form of a graph as to the effect of AC current penetration at different frequencies on different materials[59]. The results for this are presented in Figure 4.10 and Figure 4.11 and discussed in Chapter 4.

- The XY-controller that was used in the previous study by the author was split up into three separate boards for improved measurement capability. This resulted in a high-speed interface to the PC using a PC-14 card on the PC side, and two STP control and measurement units. The high-speed interface acted as the master in the PIC based embedded system. The X and Y directions are controlled by the STP controllers and the Z controller was unchanged. The amount of data that is sent to the PC for each measurement point increased from three bytes to five bytes, because the two STP readings in the X and Y directions are now also included. The immediate effect of this was that all the microcontrollers could now be run at 33MHz again. Even the Z control loop was now again running at a faster than 60kHz execution speed.

- The STP controllers were designed in such a way that they could be used again for other projects. All the peripherals are brought out to the header connectors. The PC board also fits exactly into an off the shelf enclosure. This will help if it is to be used as say as an induction motor controller. The PWM outputs will be used in this case to generate the sine waves, the two ADCs along with the interrupt inputs, the serial port and timer units will make a formidable motor controller. The STP control boards can be seen in Figure 6.10.

- Extensive testing was done with the old XY controller before it was decided that it was creating a bottleneck in the system. It was doing too many tasks (X control, Y control, STP measurement and data transmission to the PC) for it to be good at any one task. This was the main reason for splitting the XY controller into three separate parts. An attempt was made to improve the code efficiency before this system was split.

- A faster device driver was ordered for the new high-speed communications interface. The old device driver read the data three times and then only took the third set as a valid set. The reason for this was the slow response of the opto-couplers that were used. (2 μs rise time). They were replaced with fast digital opto-couplers (6N137) which enable a three fold increase in the rate that data is sent to the PC. The help of Bernard Kuc is again acknowledged in the work with the device driver. The existing driver code was just recompiled after the extra read 'for-loop" was removed. In Chapter 4, the reason for reading the data three times before using it was explained.

  The limiting factor at this point was the speed of the PC bus and hence the rate at which data could be read using the device driver. A PC with a faster bus speed will result in faster scans of the specimens. There is a limit to the fastest speed possible, but that is determined by the piezo tube. The piezo tube has a first resonant frequency at 10 kHz in the XY direction, and it has a time constant that would force the scan electronics to wait a short time before sending the data. The current configuration of the control electronics does not have the communications link between PC and the embedded system as a bottleneck.

- A 50 kHz STP detector was constructed on Veroboard and tested. Results from this board were presented in Chapter 7. The photo of this board can be seen in figure 4.7.

- A 1 MHz STP detector was constructed. The circuit was constructed and tested using two signal generators. The output of the AD633 multiplier IC showed the sum frequency very easily. This new circuit diagram is shown in appendix D. The circuit board included the 10^3 gain section of the Z controller pre-amplifier. This made the signal conditioning for the STP a lot simpler because all of the amplification could be done on one PC board,

hence keeping wiring and ultimately noise to a minimum. A photograph of the PCB is shown in Figure 4.8.

- Separate programs were written in Visual C++ to split the data into topography only and STP only data files. This software also included an additional display routine to redraw the data as a line type display. This is required to determine which data sets will be post processed using a processing package.

  The software is a new addition and was deemed necessary after the problem with processing the images during the author's MTech [14]. This software enabled the images to be screened and pre-processed before it was processed on a Sun workstation.

  Replacing this software with a Labview program that gave the final images immediately, made a further improvement. This negated the need for 3 separate programs and post processing on a Sun workstation.

- The old PC software was modified to incorporate the new STP data. The data storage and the scan routines had to be rewritten. This is because the amount of data that must be read has increased. The STM data is safe in the first double word, and the STP data is saved in the next double word. There are some empty spaces generated in the data archive, but PC storage is very cheap. The Labview interface replaced this software and proved to be much better. It is giving good graphics with just a single click of the mouse, and the software is very stable. It is not producing any fatal errors that are causing the program to shut down like the Visual C++ interface did.

- The high-speed communications interface went through 2 iterations. The first was with a parallel interface to the PC and the second was using a PIC18c8720 with an RS-232 connection to the PC. Both gave the same data throughput and the PIC18 series gave a much simpler code in the end. The code used on the parallel port version pass was copied and used "as is" on the new processor except for a few register name changes. It is working the same, but can now interface directly to the serial port functions in Labview. This was the main reason for changing to the newer PIC18c8720. It has multiple serial ports that can handle both asynchronous and synchronous data streams.

Chapter 8: Conclusions

Several interesting conclusions can be drawn from the work that was done for this thesis project. Looking at the graphs in Figure 4.10 and 4.11 it is clear that the upper limit for practical STP is about 1 MHz[59]. Higher frequencies are possible because the decrease is exponential, but the difference between materials causes a smaller decrease in penetration depth for a big increase in frequency. An example of this is the difference in penetration depths of gold and silicon at 100kHz. At this frequency, it differs by about 50μm, at 10MHz the difference is about 20μm. If it were a uniform material like graphite then the images would be a lot easier to interpret. Graphite has a grainy structure, which is one of the reasons for STP in two dimensions. By applying two slightly different signals at right angles to each other it is possible to use synchronous detection to get a difference signal and use that to plot the surface potential distribution in two separate images[60, 61].

The second is that the use of multiple PIC processors proved to be difficult to integrate when it comes to synchronisation of the various tasks. As described in Chapter 6, the four PIC based devices use a synchronous serial port to communicate with each other. The complexity of the system points towards using a system that will perform all the tasks of the four PIC processors, or at the very least three of the four. In the second option, where three of the four tasks are combined, the X, Y and Z controllers would be replaced with a new Texas Instruments[49] TMS320c240X device. This DSP chip is optimised for motor control, but it has very useful peripherals that could be used in an STM system, like several serial ports, several ADC converters and PWM outputs. The 16 different ADCs can be used to detect voltage levels at various parts of the system, and to sample the incoming tunneling current. The PWM outputs can be filtered and will produce a sine wave that can be used as the signal generators for STP. The serial ports can be used to communicate to the PC and to other peripherals in the system if they are needed.

The inclusion of a DSP into the STM electronics is a total turn around from the previously stated remark in chapter 3, where the use of DSP processors is not recommended. This is still true in a pure STM system. The proposed DSP processor (TMS320c2407A) is a 16-bit fixed point unit and can thus still do integer only calculations as required by Tapson[33]. In the current STP system, there are too many values that must be measured in a given time period.

These signals are the tunneling current and the X potentiometric and Y potentiometric information, which must be processed within a sampling rate of 60kHz. The system can work at a high scan rate with a DSP or at a much lower speed using a single microcontroller. The approach of using four microcontrollers was easy to develop in that the Z controller needed little development time and that many routines could be used "as is" from the old XY controller software. Some routines needed minor modifications, but this approach did cut down on the development time in the end. As stated previously, the synchronisation of the serial ports to prevent two ports from driving the bus at the same time proved to be a bigger challenge than anticipated. This took up a lot of time, because four programs had to be tested and debugged at the same time. When a fast scan speed is required, it is suggested that a DSP be used, especially if many measurements have to be taken.

This project delivered a system and an initial set of results to prove that the instrument is working. There are several new questions that need to be addressed. The changes to the electronics that could still be implemented are purely cosmetic and will not really improve the system as it is configured, because the current system is working well.

Chapter 9: Future Work

The STM project at UCT will continue for several years to come. The author believes that the measurement system is now reasonably fast enough to enable any follow up work to concentrate on other areas of the development for the system.

A few new items were introduced on the wish list for future improvements to the system. The first and foremost is that the system is now approaching the stage where it is becoming a serious research tool. Below, a list of items are presented that will help in the improvement of this project.

- Integration of all the separate boxes into a single unit that is more portable. At the moment, there are three power supply boxes, of which two are essentially identical. Along with a cleanup of the various PCBs that lie loose all over the place (see figure 3.1), an improved layout of the system can be done. This will also make the system more compact.
- A finite element analysis of the complete scanner assembly would assist in the understanding of the resonant frequencies that are produced. This is very important and would ultimately define the bandwidth of the Z controller. Tapson did do a complete study of the resonance behaviour of the existing scanner[12] using direct measurements. The finite element analysis can give answers as to the ideal shape of the scanhead and the behaviour of the scanner tube when it is attached to the scanhead. The scan tube comes with a set of parameters but these are changed since the tube is clamped on one side, causing it to act as a cantilever. By doing the finite element analysis, it would be possible to try new scanhead designs very quickly, and even simulate the resonant behaviour of different piezo tubes on the existing scanhead.

The next point where more work can be done is to take further measurement readings on different materials. A large database of images must be build up that can be used for research purposes. This is very important because the STP function must be characterised over a wide range of materials to gain a good understanding of what information is obtained from each type of material. If the instrument is used every day, an understanding will develop of the shortcomings in the design of the system and the end-user can provide feedback. It is

suggested that the instrument be subjected to student use for at least a year so that the students can do the initial report on the design of a GUI and modes of operations. This is suggested to help prepare the instrument for possible commercial use. The author has spend a lot of time with the instrument, but the input from various end-users is now needed to help with the design of a user friendly STM.

References

1. G. Binnig and H. Rohrer. The Scanning Tunneling Microscope. *Sci. Amer.*, 253(50):40-46, 1985.
2. G. Binnig and H Rohrer. Scanning tunneling microscopy. *IBM J. Res. Develop.*, 30(4):355-369, 1987.
3. Office of the Nobel Foundation, Box 5232, S-102 45, Stockholm, Sweden.
4. Russel Young, John Ward and Fredric Scire. The Topographiner : An Instrument for Measuring Surface Microtopography. *Rev. Sci. Instrum.*, 43(7):999-1011, 1972.
5. G. Binnig and H. Rohrer. Scanning Tunneling Microscopy. *Helv. Phys. Acta.*, 55:726,1982.
6. Ch. Gerber, G. Binnig, H. Fuchs, O. Marti, H. Rohrer. Scanning tunneling microscope combined with a scanning electron microscope. *Rev. Sci. Instrum.*, 57(2):221-224, 1986.
7. Robert D. Braun. Scanning Tunneling Microscopy of Silicon and Carbon. *J. Chem. Edu.*, 69(3):A90-A93, 1992.
8. NanoSurf AG, Grammatstrasse 14, CH-4410 Liestal, Switzerland.
9. D.W. Pohl. Some design criteria in scanning tunneling microscopy. *IBM J. Res. Develop.*, 30(4):417-427, 1986.
10. C.D. Bugg and P.J. King. Scanning capacitance microscopy. *J. Phys. E: Sci. Instrum.*, 21:147-151, 1988.
11. P. Muralt and D.W. Pohl. Scanning tunneling potentiometry. *Appl. Phys. Lett.*, 48(8):514-516, 1986.
12. G. Binnig, C.F. Quate and Ch. Gerber. Atomic Force Microscope. *Phys. Rev. Lett.*, 56(9):930-933, 1986.
13. J. Tapson. A Wide-Area Scanning Tunneling Microscope Configured for Metallurgical Research. Ph.D thesis, University of Cape Town, 1994.
14. A.H. Bredekamp. New feedback control for a scanning tunneling microscope, MTech thesis, Cape Technikon, 1998.
15. R.H.M. Groeneveld, Th. Rasing, L.M.F. Kaufmann, E. Smalbrugge, J.H. Wolter, M.R. Melloch and H. van Kempen. New optoelectronic tip design for ultrafast scanning tunneling microscopy. *J. Vac. Sci. Technol. B*, 14(3):861-863, 1996.
16. U.D. Keil, J.R. Jensen and J.M. Hvam. Transient measurements with an ultra fast scanning tunneling microscope. *Appl. Phys.*, A 66: S23-S26, 1998.

17. D.Botkin, S. Weiss, D.F. Ogletree, J. Beeman M. Salmeron and D.S. Chemla. Design considerations in an ultrafast scanning tunneling microscope. *Rev. Sci. Instrum.*, 66 (8):1894-1897, 1995.

18. A.P. Stamp, G.C. McIntosh, and Xue-Wen Liu. Current characteristics for the scanning tunneling microscope. *J. Vac. Sci. Technol. B.*, 12(3): 2175-2178, 1994.

19. J.S. Villarrubia. Morphological estimation of tip geometry for scanned probe microscope. *Surf. Sci.*, 321:287-300, 1994.

20. V. Weinstein, M. Slutzky, A. Arenshtam, and E. B. Jacob. A method for the preparation of Pt-Ir tips for the scanning tunneling microscope. *Rev. Sci. Instrum.*, 66 (4):3075-3076, 1995.

21. A.I. Oliva, A. Romero G., and J.L. Peña, E. Anguiano and M. Aguilar. Electrochemical preparation of tungsten tips for a scanning tunneling microscope. *Rev. Sci. Instrum.*, 67 (5):1917-1921, 1996.

22. R. Kazinczi, E. Szöcs, E. Kálmán and P. Nagy. Novel methods for preparing EC STM tips. *Appl. Phys.*, A 66: S535-S538, 1998.

23. STM and AFM systems from TopoMetrix Corporation. 5403 Betsy Ross Drive, Santa Clara, CA 95054-1162, USA.

24. J. Becker. Scanning tunneling microscope computer automation. *Surf. Sci.*, 181:200-209, 1987.

25. A.H. Bredekamp and J. Tapson. A scanning tunneling microscope control system based on fast microcontrollers. In *COMSIG'98: IEEE Conf. on Communications and Signal processing*, P225-228, Cape Town, South Africa, September 1998.

26. D. Jeon and R.F. Willis. Feedback system response in a scanning tunneling microscope. *Rev. Sci. Instrum.*, 62 (6): 1650-1651, 1991.

27. J.W. Gerritsen, E.J.G. Boon, G. Janssens and H. van Kempen. Design of a simple high-resolution scanning tunneling microscope with an analogue generator. *Appl. Phys.*, A 66:S79-S82, 1998.

28. J. Valenzuela-Benavides. An X-Y scan generator for a scanning tunneling microscope. *Rev. Sci. Instrum.*, 65 (8): 2733-2734, 1994.

29. Oxford Instruments. Old Station Way, Eynsham, Witwney, Oxon, OX81 TL, UK.

30. T.M.H. Wong and M.E. Welland. A digital control system for scanning microscopy and atomic force microscopy. *Meas. Sci. Technol.*, 4: 270-280, 1992.

31. D.R. Baselt, S.M. Clark, M.G. Youngquist, C.F. Spence and J.H. Baldeschwieler. Digital signal processor control of control of scanned probe microscopes. *Rev. Sci. Instrum.*, 64(7):1874-1882, 1993.

32. F.M. Battiston, M. Bammerlin, Ch. Loppacher, M. Guggisberg, R. Lüthi, E. Meyer, F. Eggimann and H.J. Güntherodt. Combined scanning tunneling and atomic force microscope with fuzzy controlled feedback. *Appl. Phys. A*, 66:S49-S53, 1998.

33. J. Tapson. Stochastic resonance and cooperative behaviour in scanning probe microscopy. *Appl. Phys. A*, 66:S17-S22, 1998.

34. K. Kajimura, H. Bando, K. Endo, W. Mizutani, H. Murakami, M. Okano, S. OkaYama, M.Ono, Y. Ono, H. Tokumoto, F. Sakai, K. Watanabe and S. Wakiyama. Construction of an STM and the observation of 2H-$NbSe^2$ atomic images. *Surf. Sci.*, 181:165-173, 1987.

35. C.W. Snyder and A.L. de Lozanne. Concentric tube tunneling microscope. *Rev. Sci. Instrum.*, 59 (4):541-544, 1988.

36. A.P. Fein, J.R. Kirtley, and R.M. Feenstra. Scanning tunneling microscopy for low temperature, high magnetic field, and spatially resolved spectroscopy. *Rev. Sci. Instrum.*, 58 (10):1806-1810. 1987.

37. B. Paillard and R. Tang and P. Rowntree. Digital linearization and cancellation of capacitive coupling for a scanning tunneling microscope. *Rev. Sci. Instrum.*, 69 (4):1770-1780, 1998.

38. A. Brown and R.W. Cline. A low cost, high performance imaging system for scanning tunneling microscopy. *Rev. Sci. Instrum.*, 61(5):1484-1489,1990.

39. G.E. Poirier and J.M. White. Diffraction grating calibration of scanning tunneling microscope piezoscanners. *Rev. Sci. Instrum.*, 61(12):3917-3920, 1990.

40. H.M. Marchman and G.C. Wetsel, Jr. Optically guided large-nanostructure probe. *Rev. Sci. Instrum.*, 64(5):1248-1252,1993.

41. K.Habib and A. Abdullah. Scanning tunneling microscopy of a magnetic shielding material in amorphous and in crystalline forms. *J. Mat. Sci. Lett.*, 9:1055-1057,1990.

42. Microsoft Corporation. One Microsoft Way, Redmond, Washington 98052-6399 USA.

43. C. Barchesi, A. Cricenti, R. Generosi, C. Giammichele, M. Luce and M. Rinaldi. A flexible implementation of scanning probe microscopy utilizing a multifunction system linked to a PC-Pentium controller. *Rev. Sci. Instrum.*, 68 (10):3799-3802, 1997.

44. National Instruments. 11500 N. Mopac Expwy, Austin TX 78759-3504, USA.

45. J.R. Kirtley, S. Washburn and M.J. Brady. Direct Measurement of Potential Steps at Grain Boundaries in the Presence of Current Flow. *Phys. Rev. Lett.*, 60(15):1546-1549, 1988.

46. J.P Pelz and R.H. Koch. Extremely low-noise potentiometry with a scanning tunneling microscope. *Rev. Sci. Instrum.*, 60(3):301-305, 1989.

47. P. Muralt, D.W. Pohl, and W. Denk. Wide-range, low-operating-voltage, bimorph STM: application as potentiometer. *IBM J. Res. Develop.* 30(5):443-450, 1986.

48. Data Translation Inc., 100 Locke Drive, Marlboro, MA, 01752-1192, USA.

49. http://www.ti.com/ is the web address for Texas Instruments. They are the manufacturers of a large range of DSP products.

50. Analog Devices, Corporate Headquarters, One Technology Way, P. O. Box 9106, Norwood, MA 02062-9106, USA.

51. http://www.intel.com/ is the corporate website address for the Intel Corporation. They manufacture a large range of microcontrollers and microprocessors.

52. Microchip Technology Inc., 2355 West Chandler Blvd., Chandler, AZ 85224-6199, USA.

53. Amor Paracherla, Implementing IIR Digital Filters, *Appl. note*, AN540.

54. Eagle Technology, P.O Box 4376, Cape Town, 8000, South Africa.

55. CI Lang and J. Tapson. Resitometric Mapping Using a Scanning Tunneling Microscope, *Mat. Res. Soc. Symp.*,500:15-20,1998.

56. J Tapson and J.R.Greene, Two-Dimensional Scanning Tunneling Potentiomentry, Proc. *Elec. Micro. Soc. of SA*, 24:14, 1994.

57. J. Tapson and J.R. Greene, Two-Dimensional Scanning Tunneling Potentiometry, *Proc. RMS* 29, 4:229, 1994.

58. F. Demming, K. Dickman, J. Jersch, Wide bandwidth transimpedance preamplifier for a scanning tunneling microscope, *Rev. Sci. Instrum.*, 66(6):2406-2408, 1998.

59. A.H. Bredekamp and J. Tapson. High Frequency Scanning Tunneling Potentiometry. In proceedings of *MSSA '99: Microscopy Soc. Of SA conf.*, Bloemfontein, South Africa, December 1999.

60. A.H. Bredekamp and J. Tapson, A low cost, high performance, modular scanning tunneling microscope control system. In preliminary proceedings of *STM '99: Int. conf. on STM*, Seoul, Korea, July 1999.

61. A.H. Bredekamp and J. Tapson. A Scanning Tunneling Microscope Control System with Potentiometric Capability. In Proceedings of *Africon '99: IEEE Int. conf.*, Cape Town, South Africa, September 1999.

62. Conversations with Mr. Andreas Tonin. Lead analogue design engineer, Institute for Physics, University of Basel, Switzerland.

Appendix A: Schematic diagram of the High speed communications interface

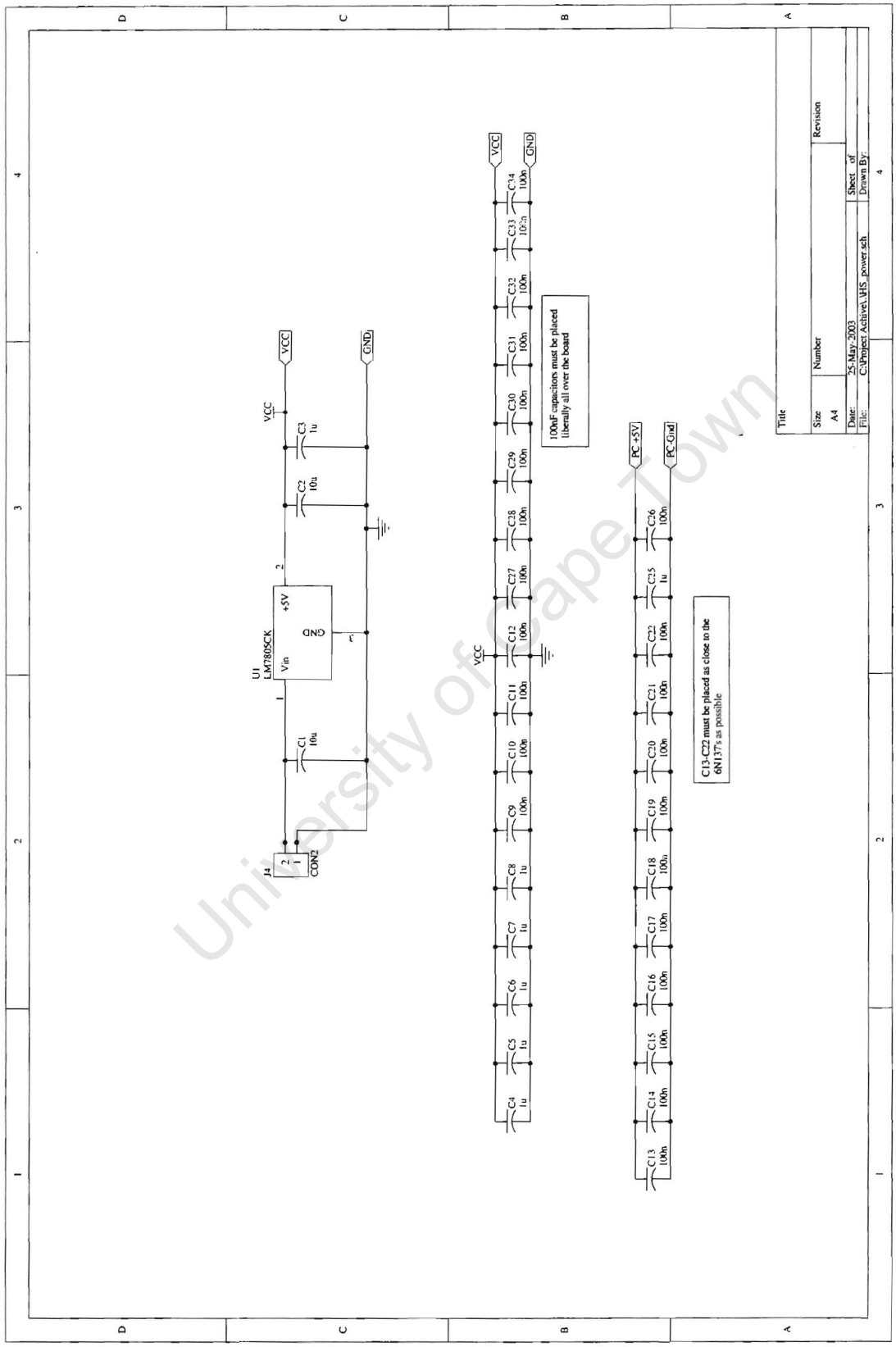

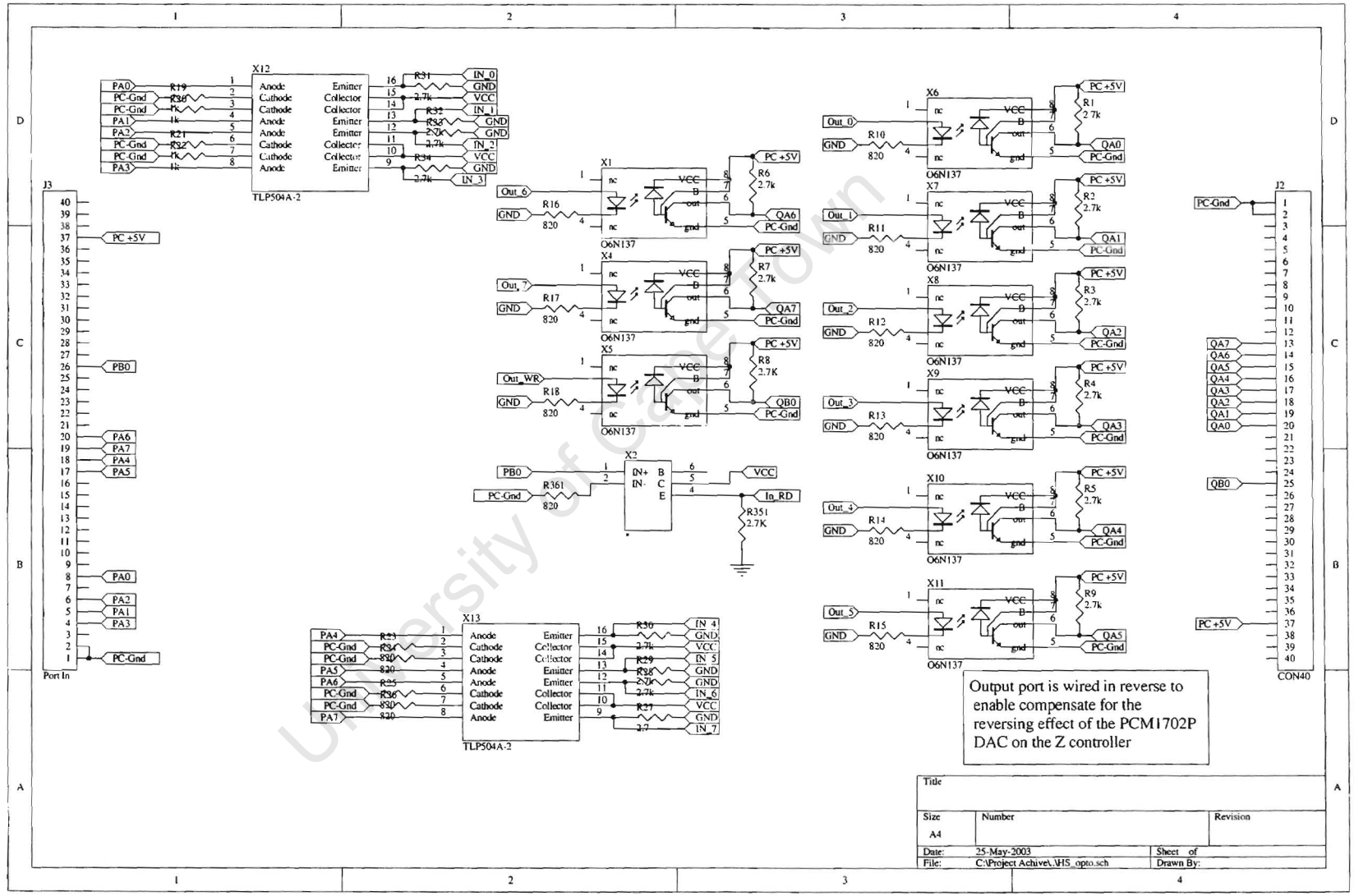

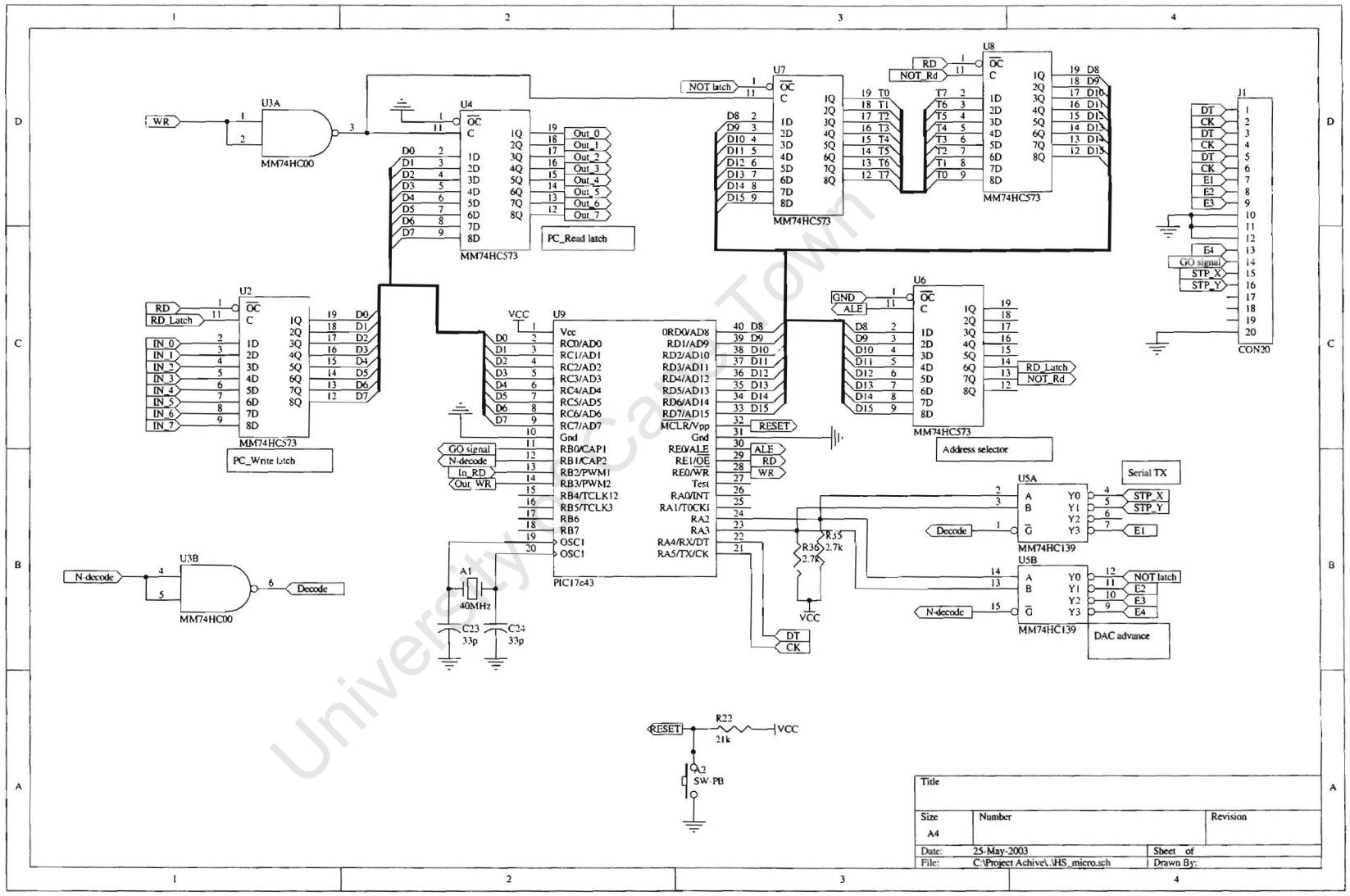

Appendix B: Schematic diagram of the STP measurement boards

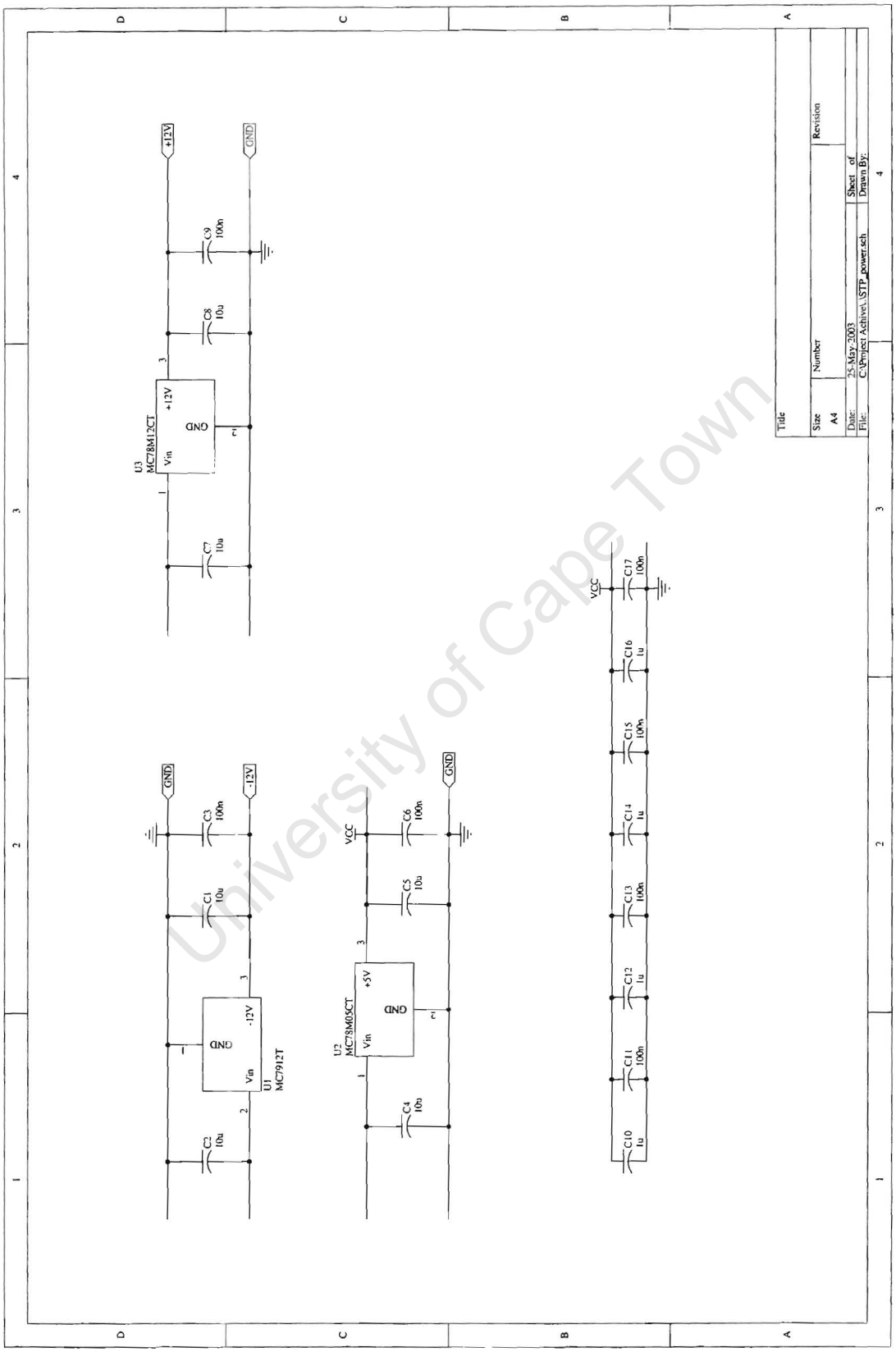

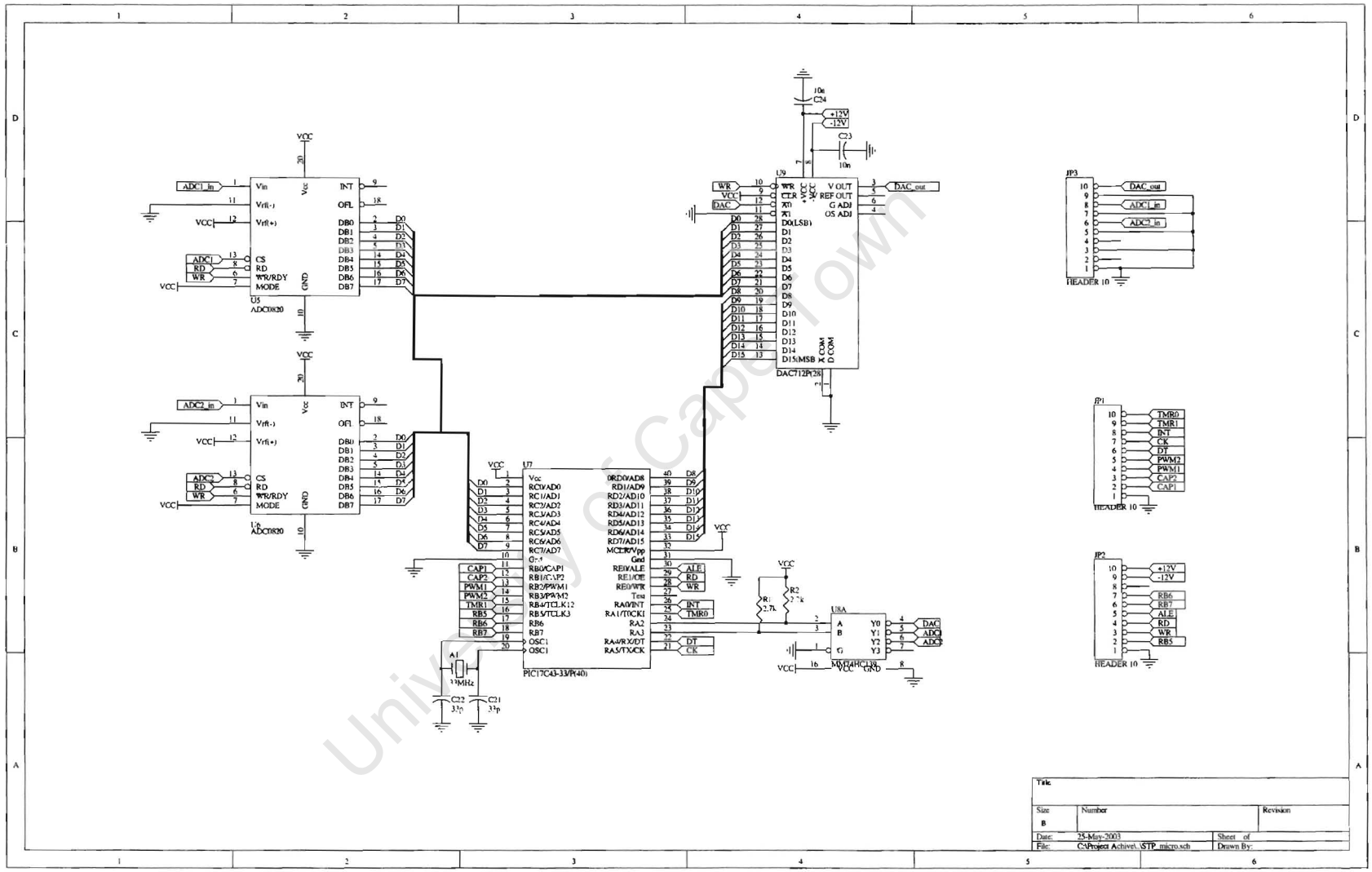

Appendix C: Schematic diagram of the new low leakage current, wide bandwidth pre-amplifier

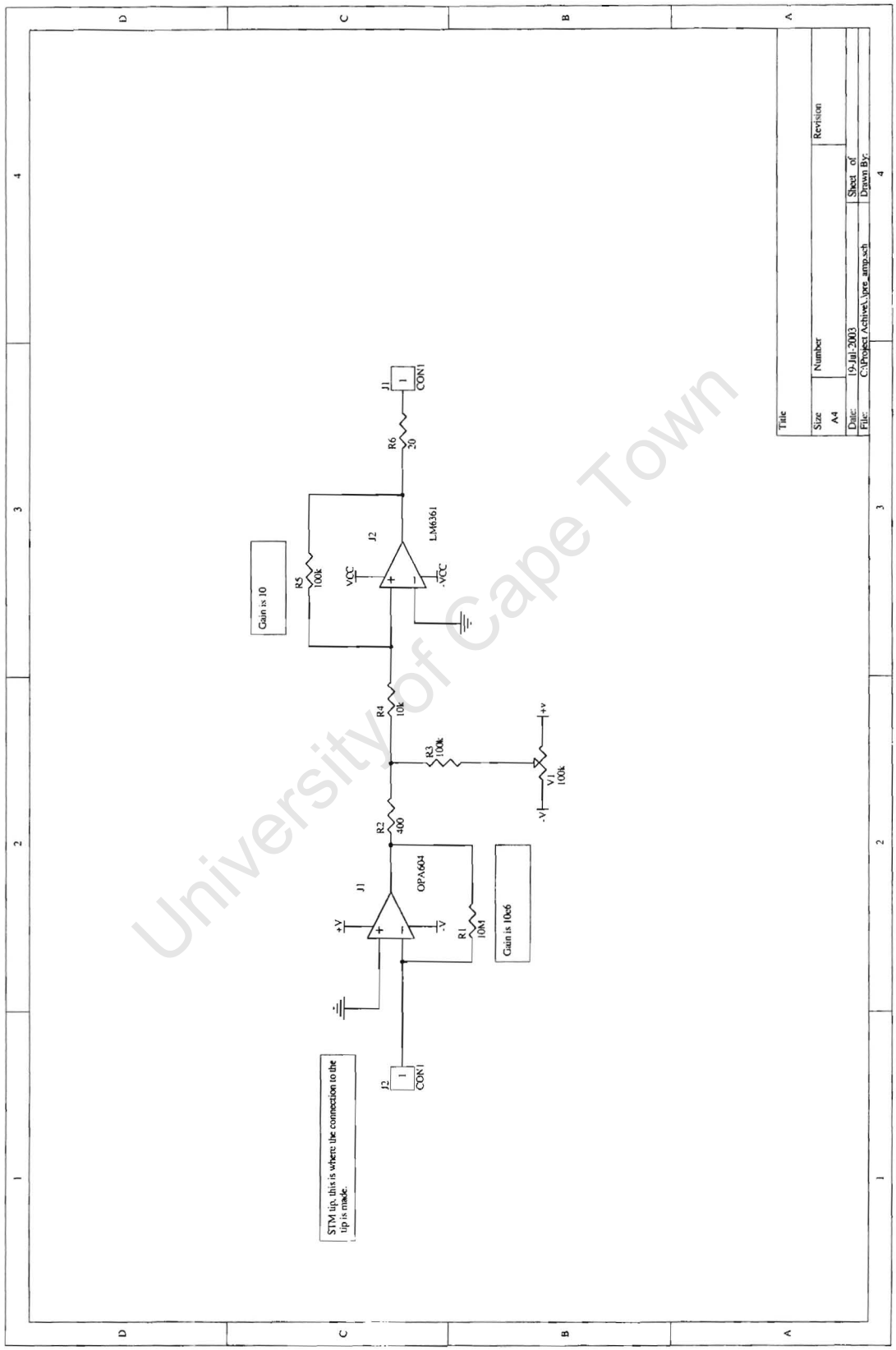

Appendix D: Schematic diagram of the 1 MHz STP detector

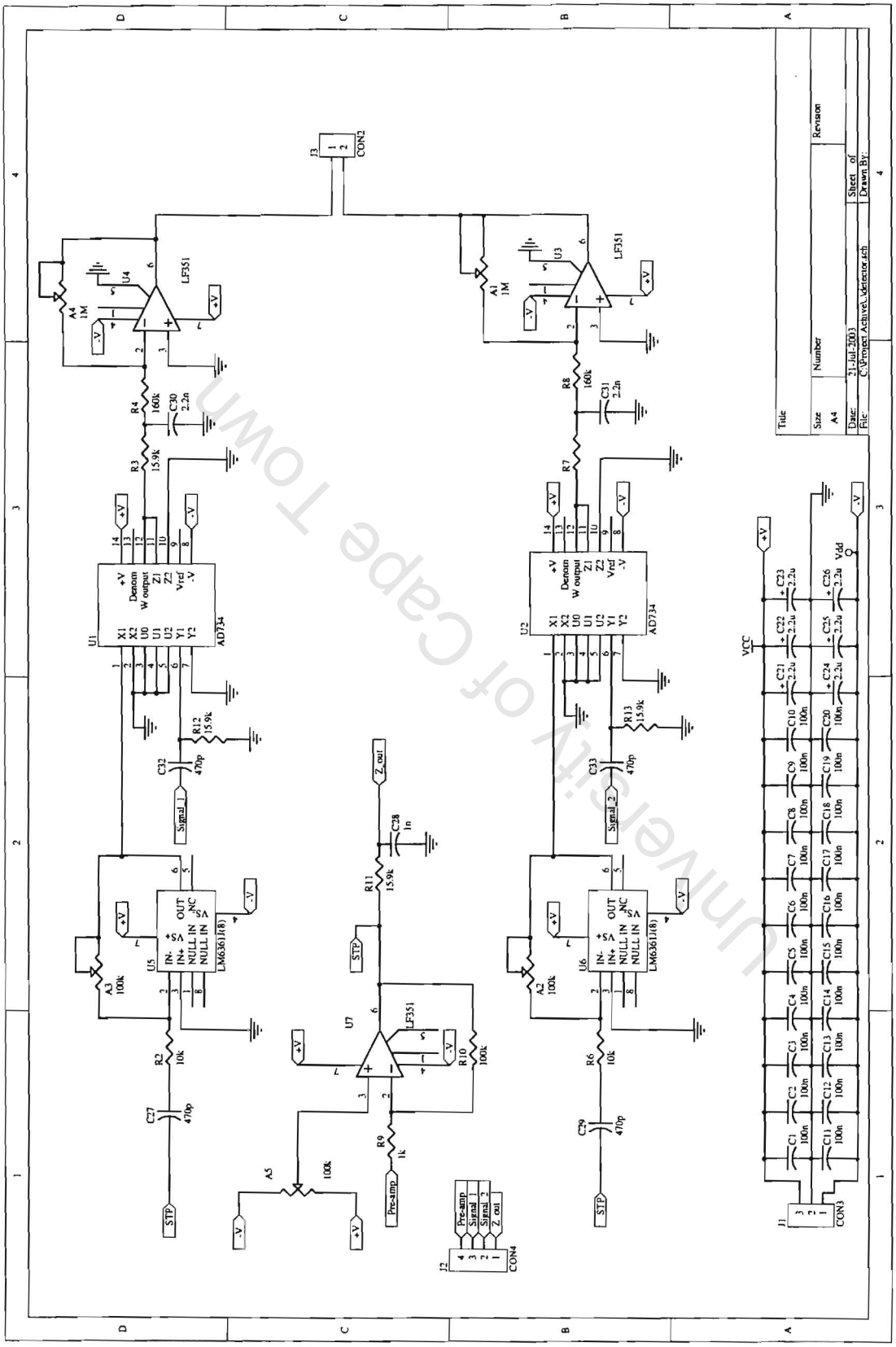

Appendix E: New PIC18c8720 board for the high speed communications interface version 2

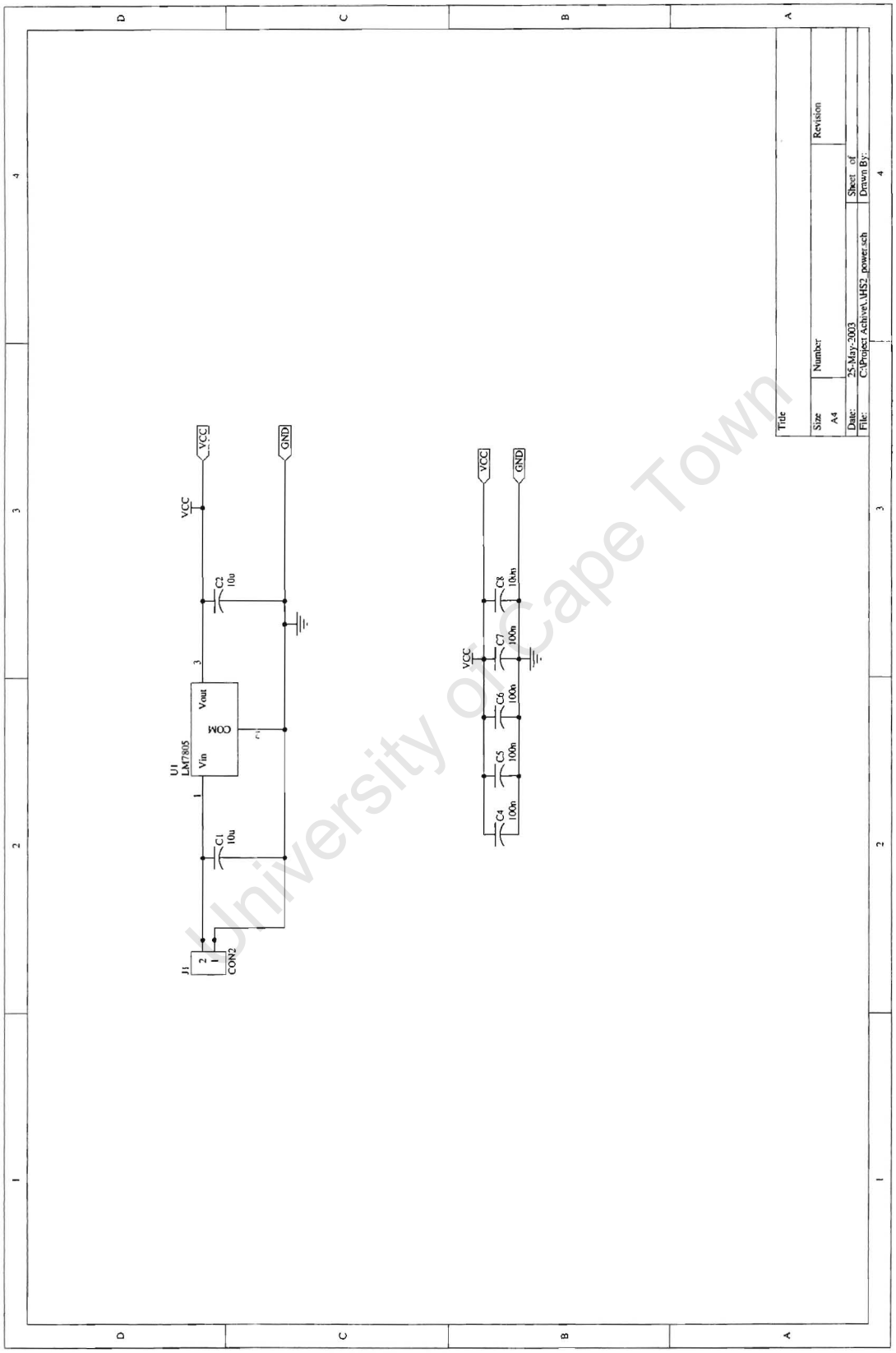

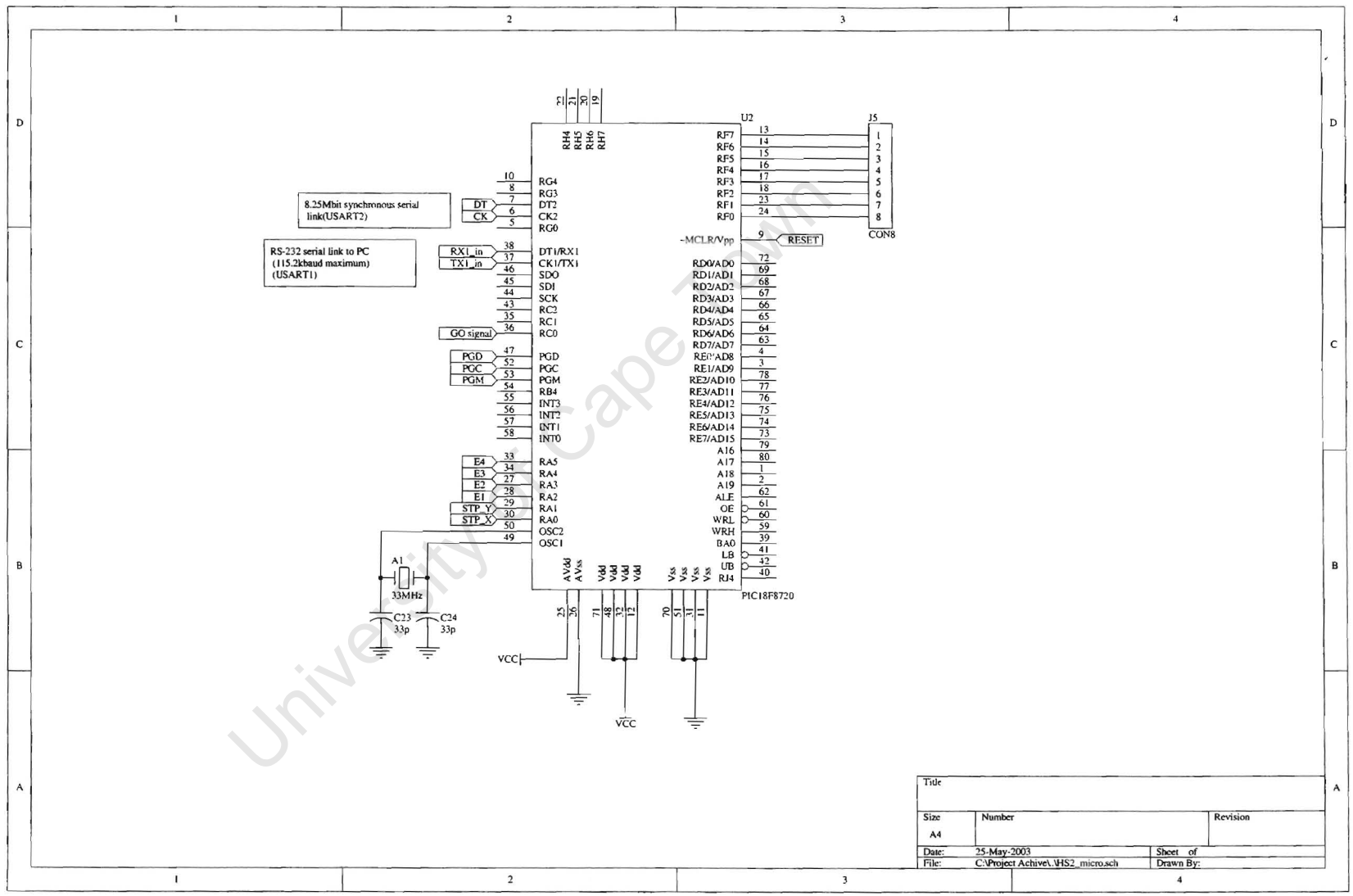

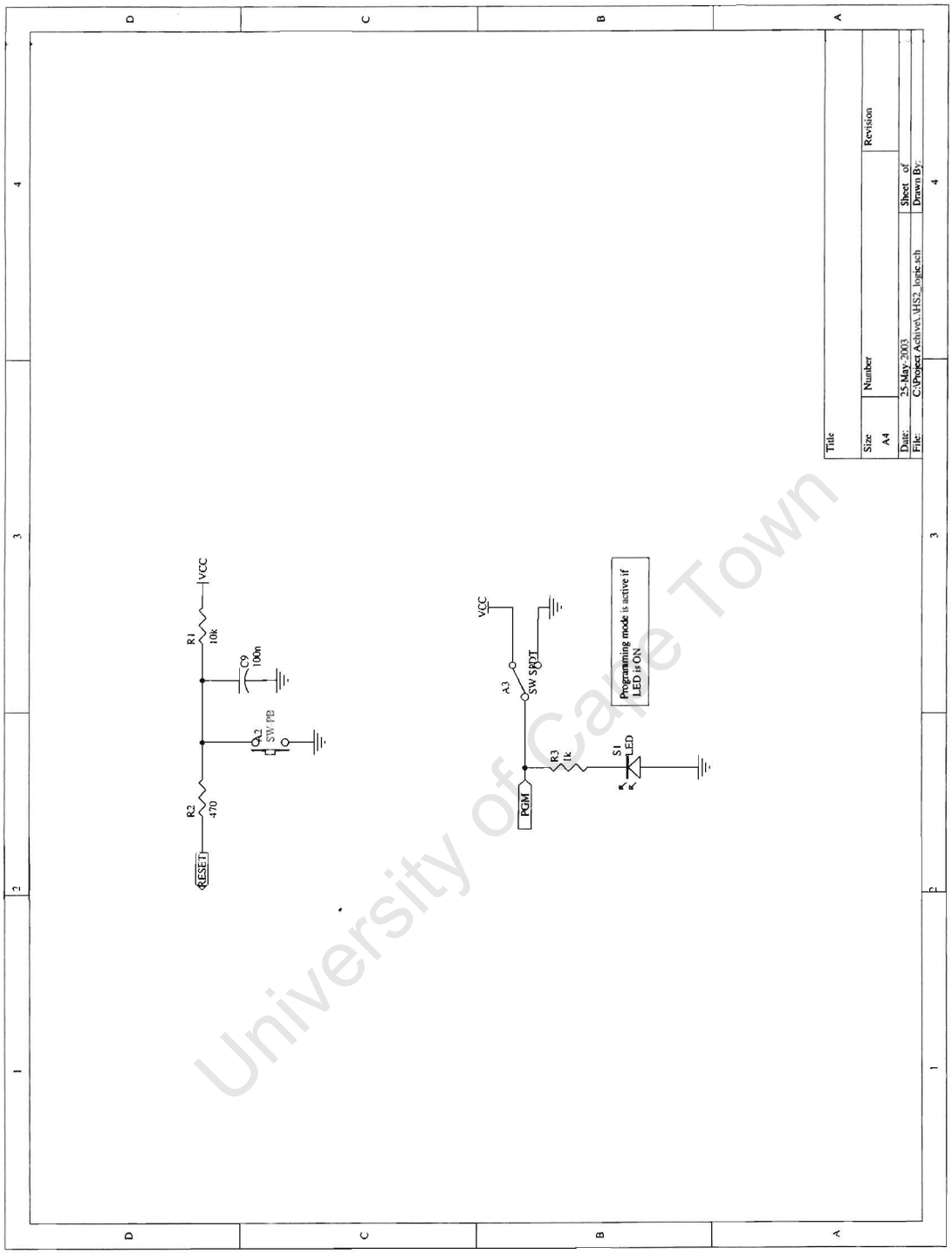

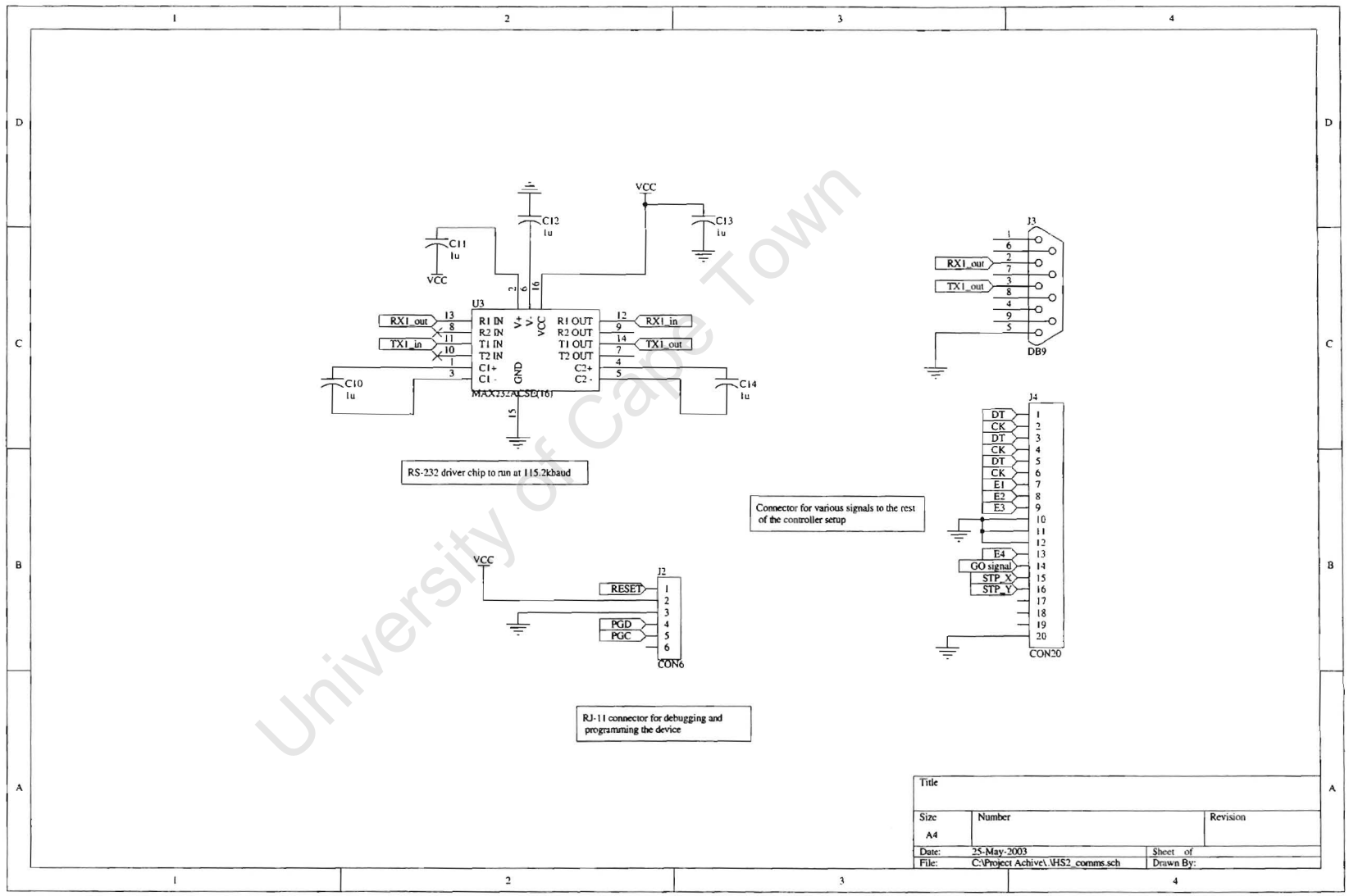

Appendix F: CD-Rom containing all the source code.